A TRIDENT SCHOLAR PROJECT REPORT

NO. 518

Electrochemical and Spectroscopic Investigations of Bismuth Ions with Sulfur-Containing Biomolecules

by

Midshipman 1/C Jonathan J. Huang, USN

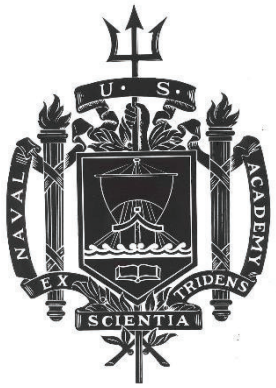

UNITED STATES NAVAL ACADEMY
ANNAPOLIS, MARYLAND

USNA-1531-2

REPORT DOCUMENTATION PAGE

Form Approved
OMB No. 0704-0188

1. REPORT DATE *(DD-MM-YYYY)*	**2. REPORT TYPE**	**3. DATES COVERED** *(From - To)*
5-16-22		

4. TITLE AND SUBTITLE
Electrochemical and Spectroscopic Investigations of Bismuth Ions with Sulfur-Containing Biomolecules

5a. CONTRACT NUMBER

5b. GRANT NUMBER

5c. PROGRAM ELEMENT NUMBER

6. AUTHOR(S)
Jonathan J. Huang

5d. PROJECT NUMBER

5e. TASK NUMBER

5f. WORK UNIT NUMBER

7. PERFORMING ORGANIZATION NAME(S) AND ADDRESS(ES)

8. PERFORMING ORGANIZATION REPORT NUMBER

9. SPONSORING / MONITORING AGENCY NAME(S) AND ADDRESS(ES)
U.S. Naval Academy
Annapolis, MD 21402

10. SPONSOR/MONITOR'S ACRONYM(S)

11. SPONSOR/MONITOR'S REPORT NUMBER(S)
Trident Scholar Report no. 518 (2022)

12. DISTRIBUTION / AVAILABILITY STATEMENT

This document has been approved for public release; its distribution is UNLIMITED.

13. SUPPLEMENTARY NOTES

14. ABSTRACT

Bismuth complexes involving amino acids provide a model system for probing physiological interactions between bismuth and the abundant thiol-containing proteins in the digestive system, whose direct study would be prohibitively complex. Such interactions may prove beneficial in the improvement of pharmaceutical agents, especially bismuth-containing metallodrugs. Interactions of bismuth pharmaceuticals including bismuth subnitrate, bismuth subsalicylate, and bismuth citrate with sulfur-containing biomolecules such as L-cysteine and L-glutathione were investigated by voltammetry and UV-Vis spectroscopy in different pH environments to characterize the complex formation between the bismuth ion and the thiol-containing ligands. Experiments were carried out at pH 1 and 3 to mimic the acidity of stomach contents and pH 7.4, to mimic that of general physiological conditions, to identify pH effects on complex formation. Cyclic voltammetry and square wave voltammetry were employed to identify reduction potential shifts that correspond to complex formation. Similarly, UV-vis spectroscopy was used to monitor complexation at a characteristic peak that forms near the 340 nm wavelength. Analysis showed that indeed the pH, the type of thiol-containing compound, and the starting bismuth pharmaceutical had an effect on the complex formation. Lower pH's lessens the interaction of L-cysteine with bismuth(III) due to protonation effects on the thiol-containing compound.

15. SUBJECT TERMS
L-Cysteine, Voltammetry, UV-Vis Spectroscopy, Complexation, Bismuth(III) nitrate, Bismuth(III) salicylate, Bismuth(III) citrate, L-Glutathione

16. SECURITY CLASSIFICATION OF:			**17. LIMITATION OF ABSTRACT**	**18. NUMBER OF PAGES**	**19a. NAME OF RESPONSIBLE PERSON**
a. REPORT	**b. ABSTRACT**	**c. THIS PAGE**		52	**19b. TELEPHONE NUMBER** *(include area code)*

U.S.N.A. --- Trident Scholar project report; no. 518 (2022)

ELECTROCHEMICAL AND SPECTROSCOPIC INVESTIGATIONS OF BISMUTH IONS WITH SULFUR-CONTAINING BIOMOLECULES

by

Midshipman 1/C Jonathan J. Huang
United States Naval Academy
Annapolis, Maryland

_____
(signature)

Certification of Adviser(s) Approval

Professor Graham T. Cheek
Chemistry Department

_____
(signature)

_____
(date)

Professor Jamie L. Schlessman
Chemistry Department

_____
(signature)

_____
(date)

Acceptance for the Trident Scholar Committee

Professor Maria J. Schroeder
Associate Director of Midshipman Research

_____
(signature)

_____
(date)

USNA-1531-2

Abstract

Bismuth complexes involving amino acids provide a model system for probing physiological interactions between bismuth and the abundant thiol-containing proteins in the digestive system, whose direct study would be prohibitively complex. Such interactions may prove beneficial in the improvement of pharmaceutical agents, especially bismuth-containing metallodrugs. Interactions of bismuth pharmaceuticals including bismuth subnitrate (bismuth(III) nitrate), bismuth subsalicylate (bismuth(III) salicylate), and bismuth(III) citrate with sulfur-containing biomolecules such as L-cysteine and L-glutathione were investigated by cyclic voltammetry and UV-Vis spectroscopy in different pH environments to characterize the formation of complexes between the bismuth(III) ion and the thiol-containing ligands. Experiments were carried out at pH 1 and 3 to mimic the acidity of stomach contents and pH 7.4, to mimic that of general physiological conditions, in order to identify pH effects on complex formation. Cyclic voltammetry was employed to identify reduction potential shifts that accompany complex formation. Similarly, UV-Vis spectroscopy was used to monitor complexation at a characteristic peak that forms near the 340 nm wavelength. Analysis showed that indeed the pH, the type of thiol-containing compound, and the starting bismuth pharmaceutical had an effect on the complex formation. More acidic conditions lessen the interaction of L-cysteine with bismuth(III) due to protonation effects on the thiol-containing compound.

Keywords: L-Cysteine, Voltammetry, UV-Vis Spectroscopy, Complexation, Bismuth(III) nitrate, Bismuth(III) salicylate, Bismuth(III) citrate, L-Glutathione

Acknowledgments

The support of Professor Graham Cheek, Professor Jamie Schlessman, and the United States Naval Academy Chemistry Department is gratefully acknowledged. I would also like to extend my gratitude towards Professor Maria Schroeder, for her unwavering support for Midshipmen Research and the Trident Scholar Program. This project was also sponsored by the Office of Naval Research, and their contributions are gratefully recognized.

Table of Contents

Introduction

Bismuth has achieved relevance in the area of medicine due to its strong anti-microbial, anti-leishmanial, and anti-cancer properties (1-5). Bismuth derivatives such as bismuth subsalicylate (bismuth(III) salicylate) which is found in Pepto-Bismol and colloidal bismuth(III) citrate treat gastrointestinal ailments, including dyspepsia and traveler's diarrhea (4, 5). Ranitidine bismuth subcitrate is used to treat ulcers, and it is a compound demonstrated to inhibit the SARS coronavirus (6-9). Bacterial infections caused by syphilis were historically treated with bismuth, and ulcers caused by *Helicobacter pylori* bacteria are also treated by bismuth compounds (1). In fact, the eradication of *H. pylori* from an infected patient can be attributed to the bacterial uptake of bismuth (10-16). While the mechanism of action is not known extensively, bismuth affects *H. pylori's* ability to uptake iron which decreases adenosine triphosphate (ATP) levels, thus reducing its energy available for metabolic functions (12). In contrast, bismuth uptake and disposal via passive transport of this metallodrug in humans was observed (17). The toxicity of bismuth to *H. pylori* and its relatively low toxicity to humans is related to the presence of glutathione transporters in humans and their absence in *H. pylori* (18, 19). Creating metallodrugs that take advantage of the lack of glutathione transporters in *H. pylori* is an untapped potential that will allow for more effective drugs to be developed in the future.

While the metallodrugs shown in Figure 1 contain bonds between the bismuth and oxygen atoms, tightly bound complexes between bismuth(III) and sulfur atoms also occur (20-24). The amino acid cysteine contains a sulfhydryl, or thiol, group (S-H) that is electrochemically active (23-25). Molecules that contain this thiol group constitute ligands, small molecules that contain a functional group capable of forming a tight-binding complex with a partner, such as a metal ion (22). Each thiol group acts as a Lewis base by donating its lone electron pairs to the metal ion. This high-affinity complex formation explains how bismuth(III) ions are removed from the human gut (17, 18). Glutathione transporters are membrane-spanning proteins that transport the tripeptide glutathione across a lipid bilayer into or out of cells or subcellular organelles to maintain redox homeostasis. This transport function is possible because these proteins recognize glutathione which, in turn, forms a complex with metal ions, including bismuth ions through its thiol group (17, 18, 26). Thus, binding of bismuth(III), or Bi(III), to glutathione forms a complex that also binds specifically to these transporters (17, 18).

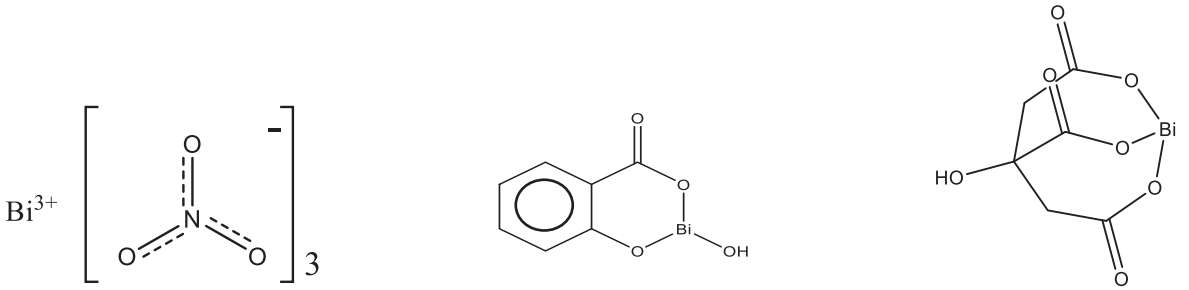

Bismuth subnitrate (BN) Bismuth subsalicylate (BSS) Bismuth citrate (BC)

Figure 1. Chemical structures for bismuth-based metallodrugs. Bismuth(III) salicylate and bismuth(III) citrate are both used to treat gastrointestinal conditions in humans. Bismuth (Bi), oxygen (O) and some hydrogen (H) atoms are depicted. Carbon atoms are located at each unlabeled vertex. Hydrogen atoms bonded to carbon atoms are not shown.

Figure 2 shows molecular structures for cysteine and glutathione. The strength of the interaction between Bi(III) and thiol-containing ligands is demonstrated by the observation that Bi(III) can be displaced from a bismuth compound and complexed to the cysteine group instead; this is due to the high affinity between the cysteine thiol group and Bi(III) (20, 21, 26). These proteins are able to complex with different types of metal ions, including bismuth ions, due to the thiol group in glutathione (24, 26). In general, sulfur-containing functional groups, in biomolecules such as cysteine and cysteine-containing compounds complex well with bismuth due to the sulfur group (25). These sulfur-containing biomolecules are an example of ligands, which contain molecules capable of acting as a Lewis base by donating its electron pairs. Cysteine undergoes such a dramatic interaction with bismuth that Bi(III) can be displaced from a bismuth compound and complexed to the cysteine group instead (23, 24). In addition, Bi(III) and cysteine complexes are able to form in harsh environments, such as strongly acidic solutions (at pH 1) (21). This is particularly useful because it allows for removal of bismuth (or "interactions of bismuth with cysteine") in the stomach, where pH ranges are typically much lower than the general physiological pH of 7.4. Changes during the complexation process can be characterized by UV-Vis spectroscopy by revealing the number of ligands involved in the process (21). For instance, bismuth(III) nitrate absorbs light at a different wavelength than does a bismuth-cysteine complex (21). Using applicable methods, the ability for bismuth ions to undergo complexation with different ligands can be determined.

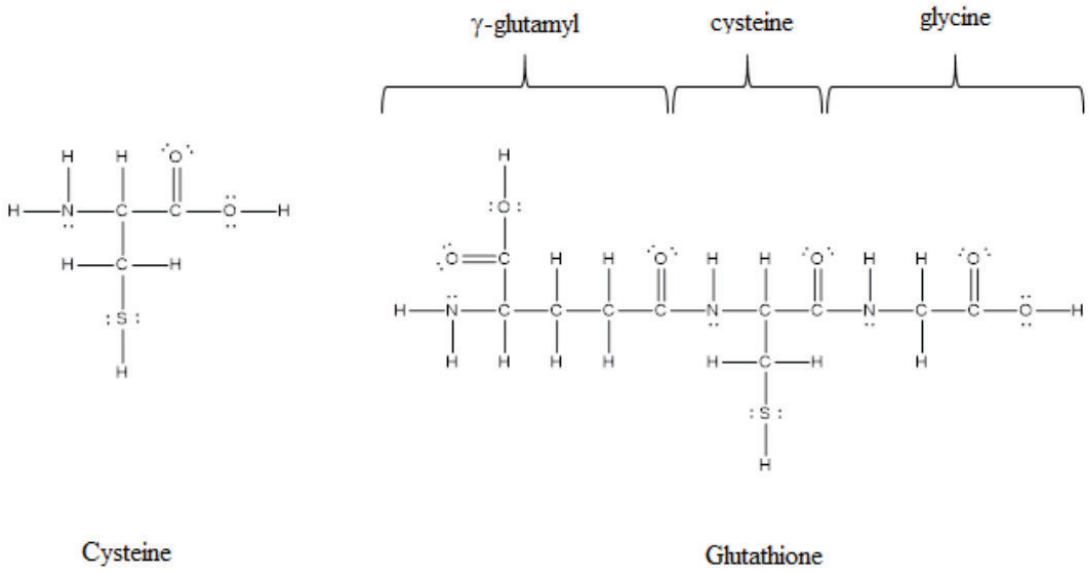

Figure 2. Chemical structures for cysteine and glutathione. Each atom is represented by a one-letter atomic symbol: carbon (C), hydrogen (H), nitrogen (N), oxygen (O), and sulfur (S). The sulfhydryl group (S-H) is electrochemically active due to its two lone pairs of electrons, each shown as a pair of dots. Glutathione is a tripeptide comprised of amino acids γ-glutamic acid, cysteine, and glycine linked through amide bonds.

Cysteine is an integral part of biological processes due to its redox properties (20, 21). In a redox process, an atom is said to be oxidized if it loses electrons and is said to be reduced if it gains electrons. Since redox processes involve electron transfer between reactants, electrochemical signals may be monitored to determine the chemical changes during cysteine complexation (20, 21). Therefore, electrochemical analytical methods such as cyclic voltammetry can be novel ways of investigating metal-ligand interactions as compared to more traditional methods such as UV-Vis spectroscopy (20, 27, 28). Qualitative and quantitative results from voltammetry will yield potential shifts during the complexation process that can be used to characterize which metal-ligand complex was created (21).

While cysteine or cysteine-containing biomolecules can operate at a range of pH values, their reactivity is highly dependent on their protonation state (26). As shown in Figure 3, cysteine's charge state shifts as the pH changes, with an overall charge of +1 in low pH ranges and neutrally charged at physiological conditions (pH 7.4) (29). Because bismuth exists as Bi(III) in pH 1.0 and BiO^+ in pH 7.4, electrostatic interactions also play a role in the interaction between Bi(III) and thiol-containing biomolecules (30).

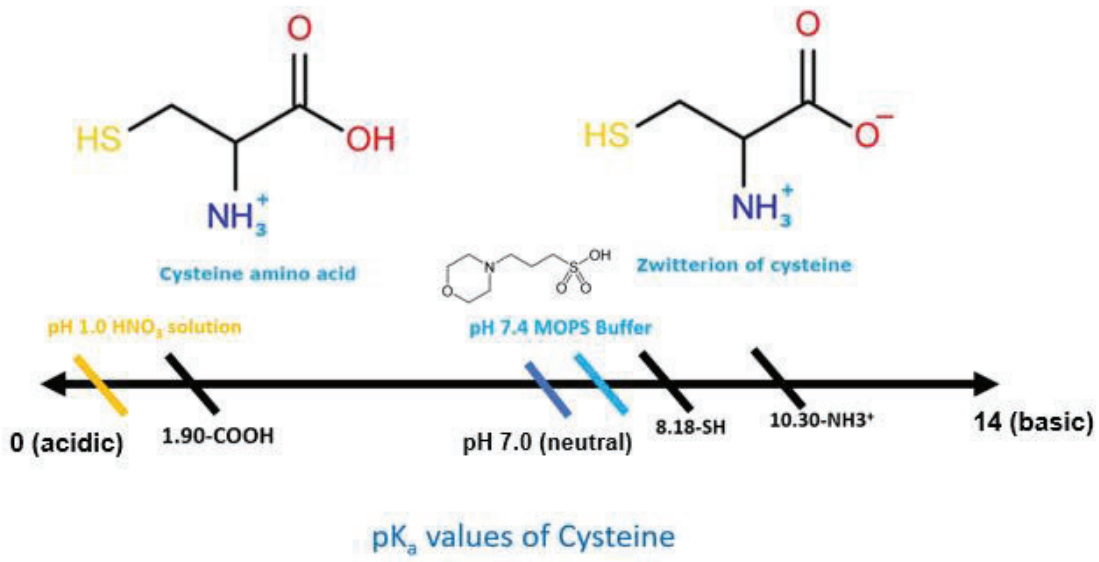

Figure 3. Protonation diagram of cysteine as a function of pH (29).

At pH 1.0, complexation involves the reaction:

$$Bi^{3+}_{(aq)} + qCysH^{+} \rightleftharpoons Bi(Cys)_q{}^{3+} + qH^{+}_{(aq)} \qquad \text{[Eq. 1]}$$

The Cys H^+ denotes the +1 charged and protonated state of L-cysteine. At pH 7.4, complexation involves the following reaction:

$$BiO^{+}_{(aq)} + 2H^{+}_{(aq)} + qCys \rightleftharpoons Bi(Cys)_q{}^{3+} + H_2O_{(l)} \qquad \text{[Eq. 2]}$$

q is the stoichiometric ratio of cysteine required to complex with Bi^{3+}. The redox behavior (reduction) at pH 1.0 involves the process:

$$Bi(Cys)_2{}^{3+} + 3\,e^{-} + 2H^{+}_{(aq)} \rightleftharpoons Bi^{0}_{(s)} + 2CysH^{+} \qquad \text{[Eq. 3]}$$

The physical processes defined by the complexation reaction and the redox behavior by Equations 1-3 can be modeled by electrochemical equations given in Equations 4 and 5 (31). Equation 4 is the Nernst equation, and it essentially states that the potential will decrease as the concentration of the ligand increases, which is denoted by the term $C_Y{}^*$. Equation 5 is the peak

current equation, which is influenced by factors such as number of electrons, n; area of the electrode surface, A; the diffusion coefficient, D_0; and the concentration of ligand, C_0^*.

$$E_{1/2} = E^0 + \frac{0.059}{n} log \frac{m_R}{m_A} + \frac{0.059}{n} logK - \frac{0.059}{n} q\ logC_Y^* \qquad \text{[Eq. 4]}$$

$$i_p = (2.69 \times 10^5) n^{3/2} A D_0^{1/2} C_0^* v^{1/2} \qquad \text{[Eq. 5]}$$

Experimental Methods

All reagents including L-cysteine, L-glutathione, bismuth(III) salicylate, bismuth(III) citrate, bismuth subnitrate, and 3-(N-morpholino)propanesulfonic acid (MOPS) were obtained from Sigma-Aldrich. Electrochemical experiments were carried out using a Gamry Interface 1000 Potentiostat, and potentials were measured versus a Ag/AgCl reference electrode (eDAQ). Glassy carbon electrodes (3 mm diameter) were obtained from Bioanalytical Systems. The glassy carbon electrodes were manually polished using Buehler 0.05 μm alumina polishing suspension on a felt polishing pad, rinsed with deionized water, then placed in a Cole-Parmer 8890 sonicator for five minutes to remove alumina particles. The electrochemical cell was a 20 mL cylindrical cell fitted with a PTFE top and 1 mm diameter platinum wire counter electrode. Bismuth compounds were added (by mass) to appropriate electrolytes to prepare 10.0 mL of a nominal 1.0 mM bismuth solution. The contents in the cell were de-aerated, or purged, with a stream of N_2 gas and stirred with a magnetic stirring bar for 10 minutes to remove oxygen from the solution and prevent unwanted oxidation of reagents (i.e., L-cysteine). The cell was cleaned by submerging the cell and its components into aqueous 0.100 M K_2EDTA solution overnight in order to remove any bismuth ions adsorbed to the glass cell walls. All experiments were carried out at 22 ± 1°C. Two sweeps were performed for each electrochemical experiment, and each electrochemical experiment was run at least twice to ensure accuracy and consistency.

An Agilent 8453 UV-Vis diode-array spectrophotometer was utilized to obtain UV-Vis spectra. 3.0 mL of the 1.0 mM bismuth solution was pipetted into a quartz cuvette (1.0 cm path length). The cell was purged of oxygen with a nitrogen stream, and the top of the cell was closed with a septum-seal cap (Starna) to isolate the sample from oxygen. 0.06 M L-cysteine solution was injected through the cap via a Hamilton microsyringe to make the various additions of L-cysteine. To confirm the spectrophotometer's sensitivity, preliminary spectra were collected on a JASCO V-670 UV-Vis spectrophotometer for comparison to data from the Agilent instrument. Three measurements were performed for each spectrophotometric experiment to ensure accuracy and consistency.

Hydrochloric acid (HCl), nitric acid (HNO_3), and MOPS buffer were the aqueous media used to set the pH environments for each experiment. pH 1.0 HCl and HNO_3 were used from the 0.10 M stock solution. pH 3.0 HCl and HNO_3 were created by diluting the 0.100 M stock solutions and adding KCl for HCl solutions and KNO_3 for HNO_3 solutions to maintain 0.100 M ionic strength. MOPS (3-N-morpholino)propanesulfonic acid) buffer solution was created and then titrated to pH 7.4 with sodium hydroxide (NaOH). Final pH values were verified through a pH meter within ± 0.02 from the target pH value. MOPS was chosen as the buffer of choice due to its relatively inert behavior in the presence of metal ions. That is, it is highly unlikely for MOPS to interact and complex with any species present in the solution (34).

Results and Discussion

Bismuth(III) nitrate (BN) in pH 1.0 in HCl, with L-cysteine additions

The nominal 1.0 mM BN solution was only slightly soluble in pH 1.0 HCl as observed by only a small stripping peak on the return sweep. The sample containing the solution was cloudy, visually indicating that the 1.0 mM BN solution was only slightly soluble. Upon the addition of the first molar equivalent of L-cysteine to the 1.0 mM BN solution, a reduction peak was observed at -0.27 V, reaching a peak current of -18.0 μA (Figure 4). A 2:1 Cys to Bi (Bi = Bi(III) ion) ratio resulted in a slightly positive reduction potential shift to -0.25 V and an even lower peak current than at the 1:1 Cys to Bi ratio. These results suggest that at 1:1 Cys to Bi, the complex between Bi^{3+} and cysteine has not fully formed yet, although chloride ions may also be complexed to the Bi^{3+} ions. This slight chloride effect results in a more negative potential when compared to the 2:1 and the 4:1 Cys to Bi ratios. At the 4:1 Cys to Bi ratio, the reduction potential is the same as the 2:1 sample, but with a greater reduction peak current of 45 μA. This result suggests that more Bi^{3+} ions are being brought into solution by the cysteine ligands. Gradual additions of L-cysteine did make the solution less cloudy, but there was not a point at which the solution became completely clear. This implies that the high proton concentration, and perhaps chloride ions, greatly impedes bismuth-cysteine complexation. In addition, the bismuth stripping region displays two peaks, the more negative of which evidently corresponds to stripping of bismuth in the presence of only chloride ion, as seen for the curve for which no L-cysteine has yet been added. As L-cysteine was added, the stripping peak at more positive potential eventually predominates, reflecting the increasing involvement of L-cysteine in bismuth complexation. The results of UV-Vis spectroscopy confirm the mixed interactions between the chloride ions and L-cysteine (Figure 5). Normally, complexes that form between L-cysteine and bismuth ions result in a characteristic absorption peak at 320-340 nm wavelength as shown in Figure 7. From the spectrum in Figure 5, it is clear that the absorption peak lies in 0.100 M HCl at around 290 nm, with a much lower absorbance than in Figure 5. The voltammetric results are supported by the observation of an ultimate reduction peak current of approximately 70 μA for a similar experiment at pH 1.00 in HNO_3 as shown in Figure 6. Thus, the cysteine-bismuth complex was not fully formed, implying that the solution contained a mixed chloro-complex solution. This finding is reasonable considering the relatively high 100 mM chloride concentration compared to the nominal 1.0 mM bismuth (III) concentration. In addition, at pH 1.00, L-cysteine is fully protonated, lowering its effectiveness as a ligand to the bismuth(III) ion.

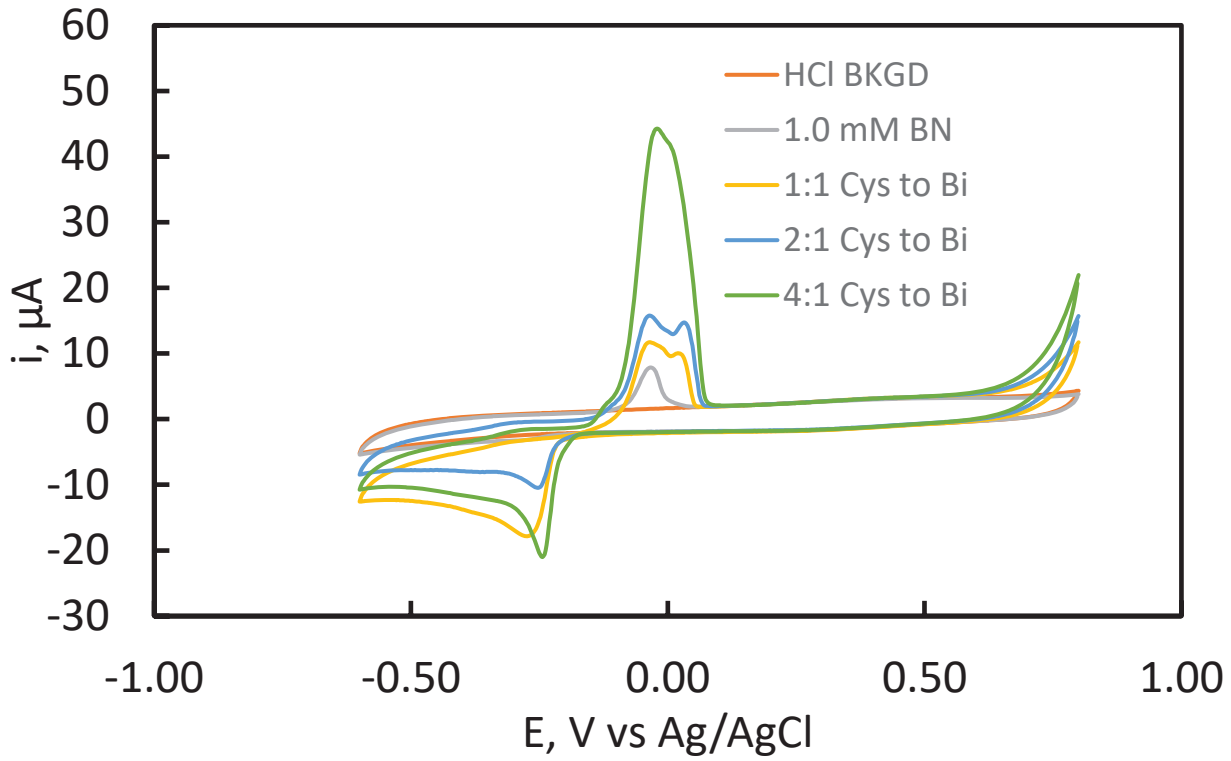

Figure 4. Cyclic voltammograms for 1.0 mM BN at glassy carbon in 0.10 HCl, 100 mV/s, showing the effects of L-cysteine additions.

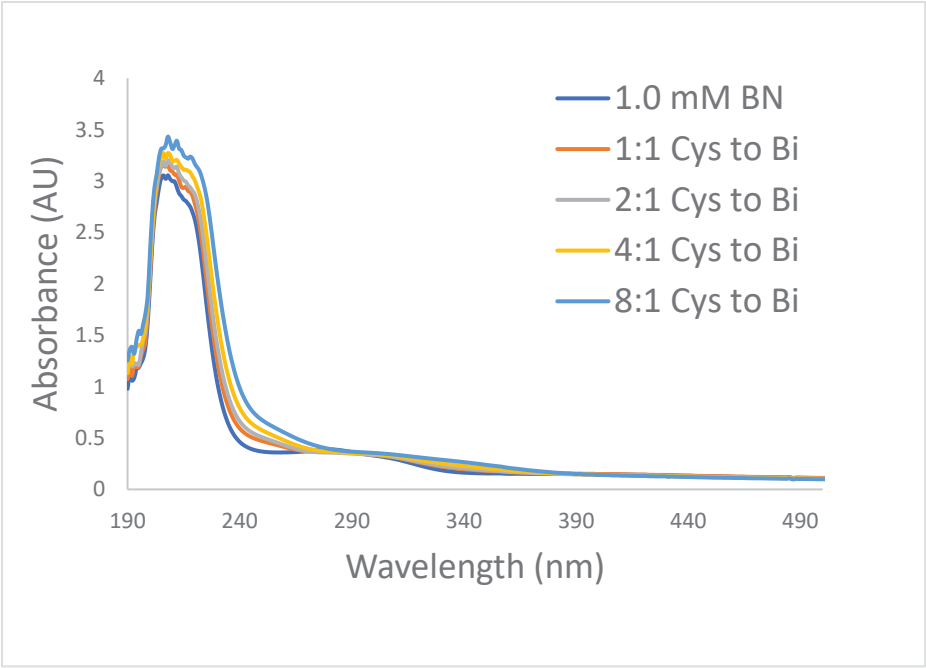

Figure 5. UV-Vis spectra of 1.0 mM BN in 0.10 M HCl, with incremental additions of L-cysteine. The path length was 1.00 cm.

Bismuth(III) nitrate (BN) in pH 1.0 in HNO_3, with L-cysteine additions

In contrast to BN in 0.10 M HCl (pH 1.0), BN in 0.10 M HNO_3 (pH 1.0) interacts more strongly with L-cysteine. Additions of L-cysteine gradually made the solution clear, with the solution being completely clear by the 8:1 ratio. The cyclic voltammograms demonstrate this effect (Figures 4 and 6). For example, Figure 4's stripping peak only reached a maximum of 50 μA for the 4:1 Cys to Bi ratio; however, Figure 6 shows that in pH 1.0 HNO_3, the maximum current for the 4:1 Cys to Bi ratio went up to 150 μA. From the differences in the magnitudes of the maximum currents for the stripping peaks, BN is more soluble in 0.100 M nitric acid than in 0.10 M hydrochloric acid, with L-cysteine additions. However, it should be noted that initially, the BN was more soluble in 0.10 M HCl than in 0.10 M HNO_3 due to the chloro-complex. The former is evidently due to a higher concentration of the completely formed Bi-cys complex in nitric acid than in hydrochloric acid. Clearly, the absence of chloride ions in nitric acid allowed the Bi-cys complex to form without any possibility for a chloro-complex to form. The nitrate anion generally shows minimal ability to form complexes with metal ions (32). The single-component stripping peak also supports this conclusion. The UV-Vis spectrum confirms the absence of any chloro-complexes due to the presence of strong absorbance peaks at 340 nm due to L-cysteine complexation (Figure 7). The cyclic voltammetric results in Figure 4 show that the effect of L-cysteine addition ceases at the 4:1 Cys to Bi point, but it is not certain that the complex actually involves four L-cysteine ligands. Although the absorption for the 340 nm peak is still increasing from the 4:1 to the 8:1 Cys to Bi point, it is difficult to account for corresponding increases in the background due to the process at 250 nm. Overall, in pH 1.0 HNO_3, the high proton concentration ensures the existence of L-cysteine in its protonated form, lowering the effectiveness of the L-cysteine as a ligand and requiring the presence of more than the stoichiometric amount of L-cysteine to form the final complex.

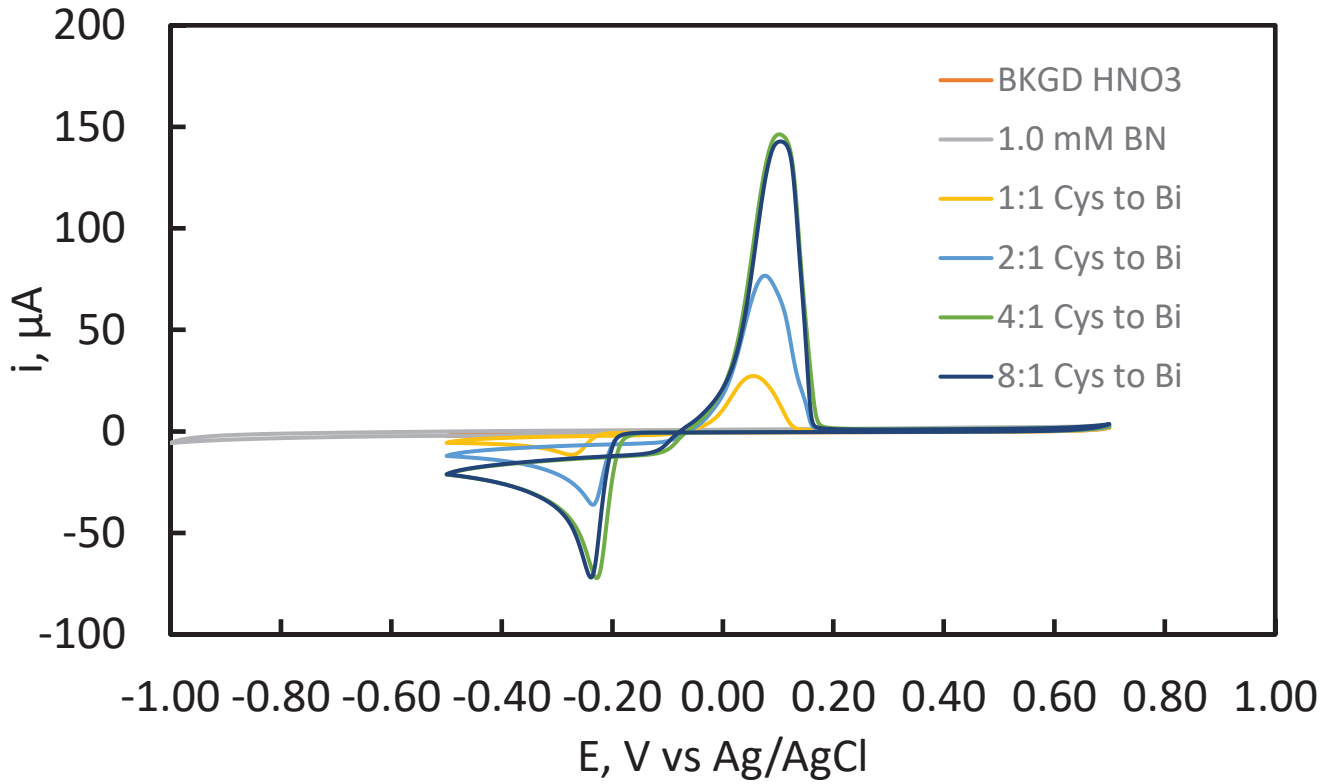

Figure 6. Cyclic voltammograms for 1.0 mM BN at glassy carbon in 0.10 M HNO_3, 100 mV/s, showing the effects of L-cysteine additions.

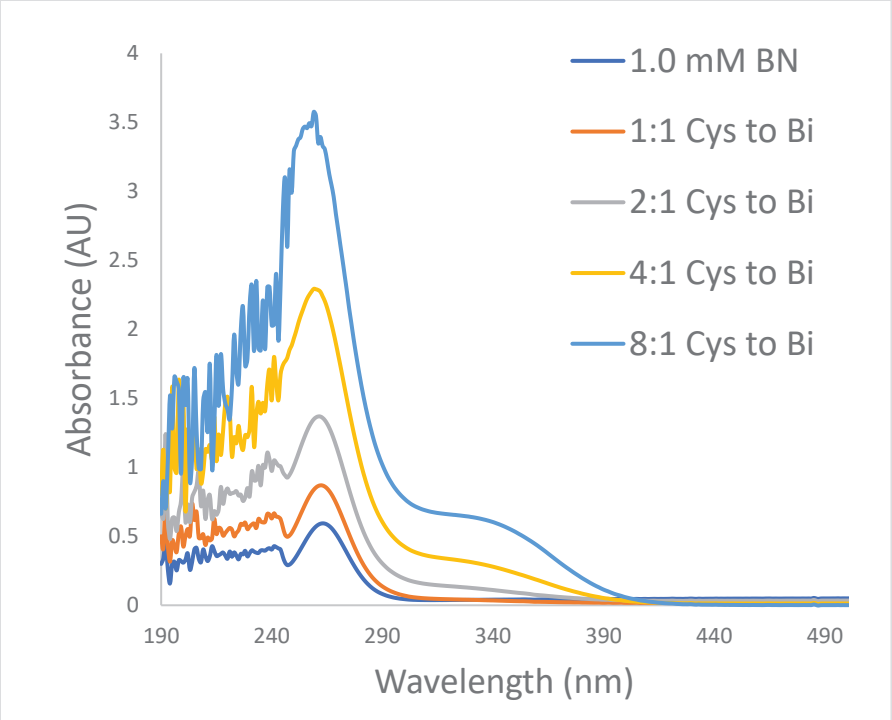

Figure 7. UV-Vis spectra of 1.0 mM BN in 0.10 M HNO_3, with incremental additions of L-cysteine. The path length was 1.00 cm.

Bismuth(III) nitrate (BN) in pH 1.0 in HCl, with L-glutathione additions

Additions of L-glutathione to BN in pH 1.0 HCl did not prevent BN from forming chloro-complexes. From the cyclic voltammograms, the profile of BN in 0.10 M HCl after L-glutathione (GSH) additions resembled the profile of BN in 0.10 M HCl after L-cysteine additions (Figures 4 and 8). Both voltammograms had a maximum stripping peak ranging from 40-50 μA, and both had low magnitudes of the current at the reduction potential (20 μA). Although the solution exhibited considerable cloudiness at all ratios of GSH to Bi, the increasing peak currents in Figure 6 show that there is considerable interaction between bismuth nitrate and added GSH. From the UV-Vis spectra, additions of L-glutathione caused small increases in the absorbance, and a corresponding small increase in the region between 300 nm and 350 nm (Figure 9). This broad response is not as pronounced as the 340 nm complexation peak in 0.10 M HNO_3 (Figure 7). This spectral behavior is similar to Figure 5 in that the absorption peak for the chloro-complexes is present with low absorption units, indicating the low concentration of Bi(III) species complexed entirely by GSH. Considering the split bismuth stripping processes in Figure 8, the formation of mixed chloride/GSH complexes is also likely in this case. The highly acidic nature of the solution may also play a role here, although the carboxylic acid and amine groups of the cysteine component are bonded to the neighboring amino acids in GSH. Again, the addition of 8:1 GSH to Bi(III) does not imply formation of a complex with eight GSH ligands, only that a high GSH

concentration is necessary to overcome the high acidity and chloride content of the solution and produce at least some GSH complexation.

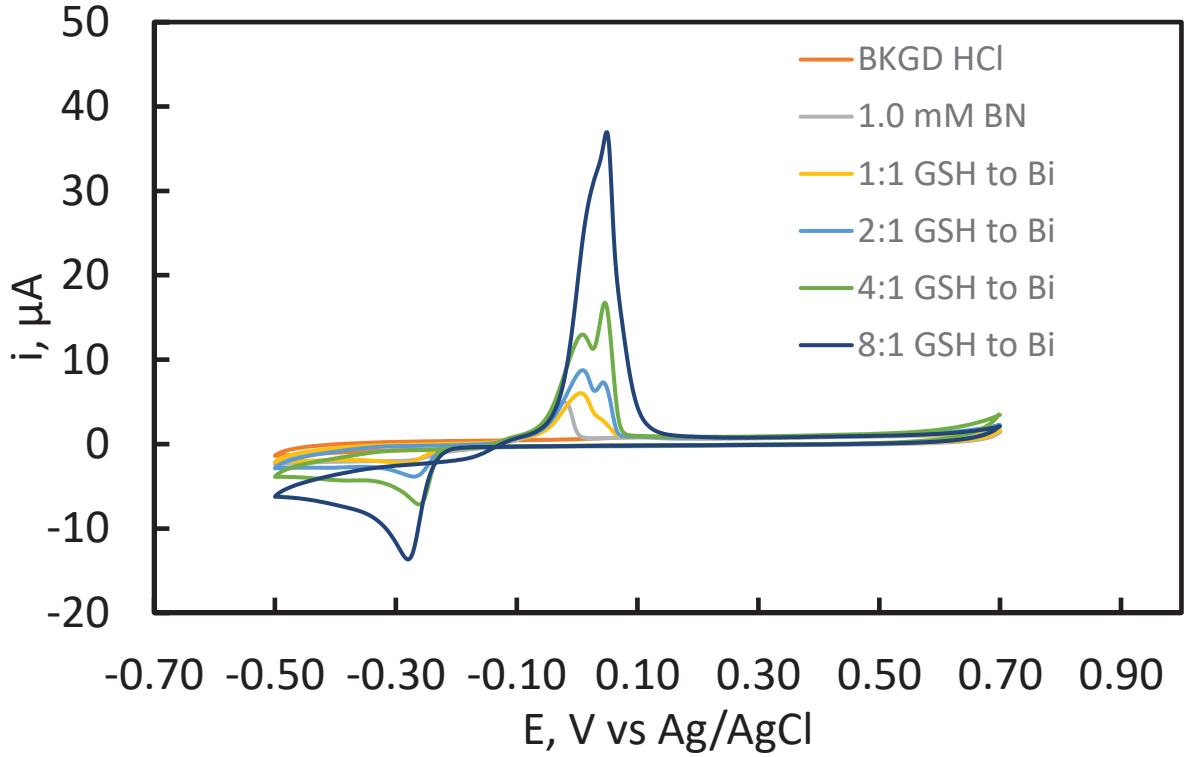

Figure 8. Cyclic voltammograms for 1.0 mM BN at glassy carbon in 0.10 HCl, 100 mV/s, showing the effects of L-glutathione (GSH) additions.

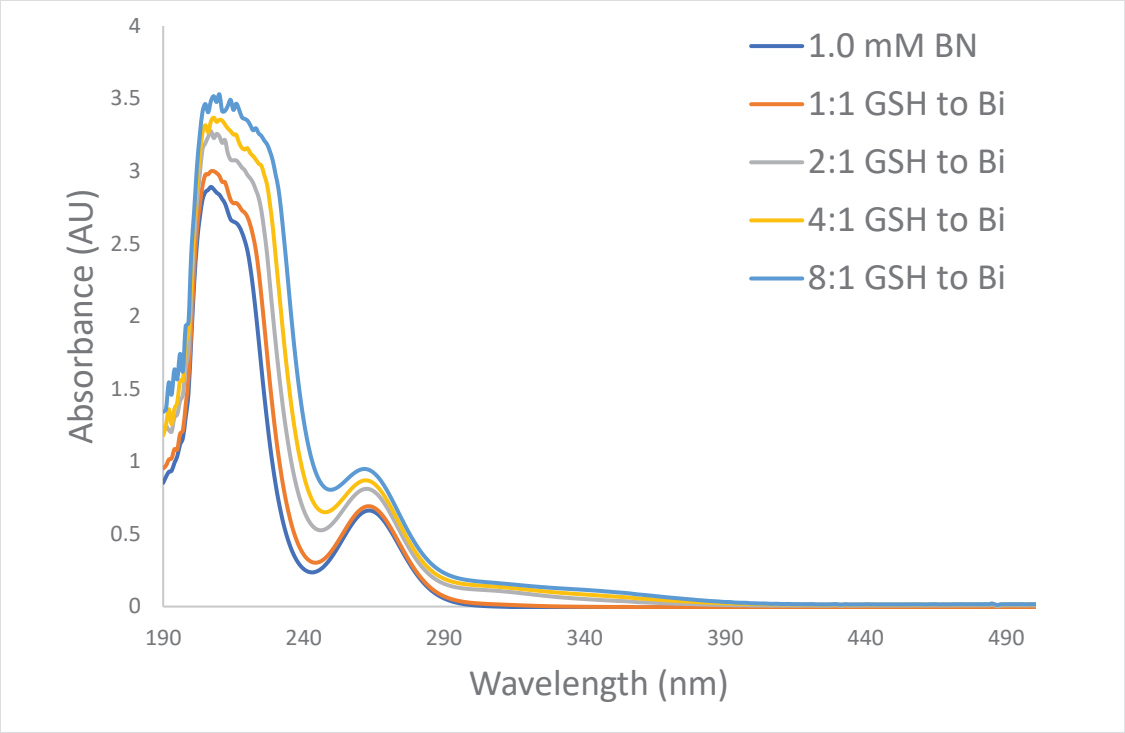

Figure 9. UV-Vis spectra of 1.0 mM BN in 0.10 M HCl, with incremental additions of L-glutathione. The path length was 1.00 cm.

Bismuth(III) nitrate (BN) in pH 1.0 in HNO_3, with L-glutathione additions

Much as in the case of BN in pH 1.0 HNO_3 with L-cysteine additions, L-glutathione (GSH) additions were able to form soluble complexes with the Bi^{3+} ions. The solution became clear after the 2:1 GSH to Bi ratio. Gradual increases in GSH caused corresponding increases in the peak current of the stripping peak and the bismuth(III) (Figure 10). Increasing the GSH concentrations drives the equilibrium towards the formation of the Bi-GSH complex, and the cyclic voltammetry indicates that complexation is complete at the 4:1 GSH to Bi point. After this point, the reduction peak currents remains constant, although there is a potential shift from -0.25 V to -0.30 V at the 8:1 GSH to Bi ratio. Such potential shifts are commonly observed for complex formation in the presence of excess ligands (31). The presence of a single bismuth stripping peak indicates that complexation is relatively uncomplicated and that only one ligand (i.e. GSH) was involved. UV-Vis spectroscopy confirms the results of cyclic voltammetry with the 340 nm wavelength complexation peak present to some extent at all ratios of GSH to Bi (Figure 11). Each subsequent increase in the GSH concentration increased the absorbance as well, paralleling the increase in maximum current for cyclic voltammetry, indicating the increase in Bi-GSH concentrations.

Therefore, in the absence of chloride ions, complexation between Bi(III) and GSH is able to occur despite the unfavorable protonation state for GSH, indicating a strong affinity for Bi(III).

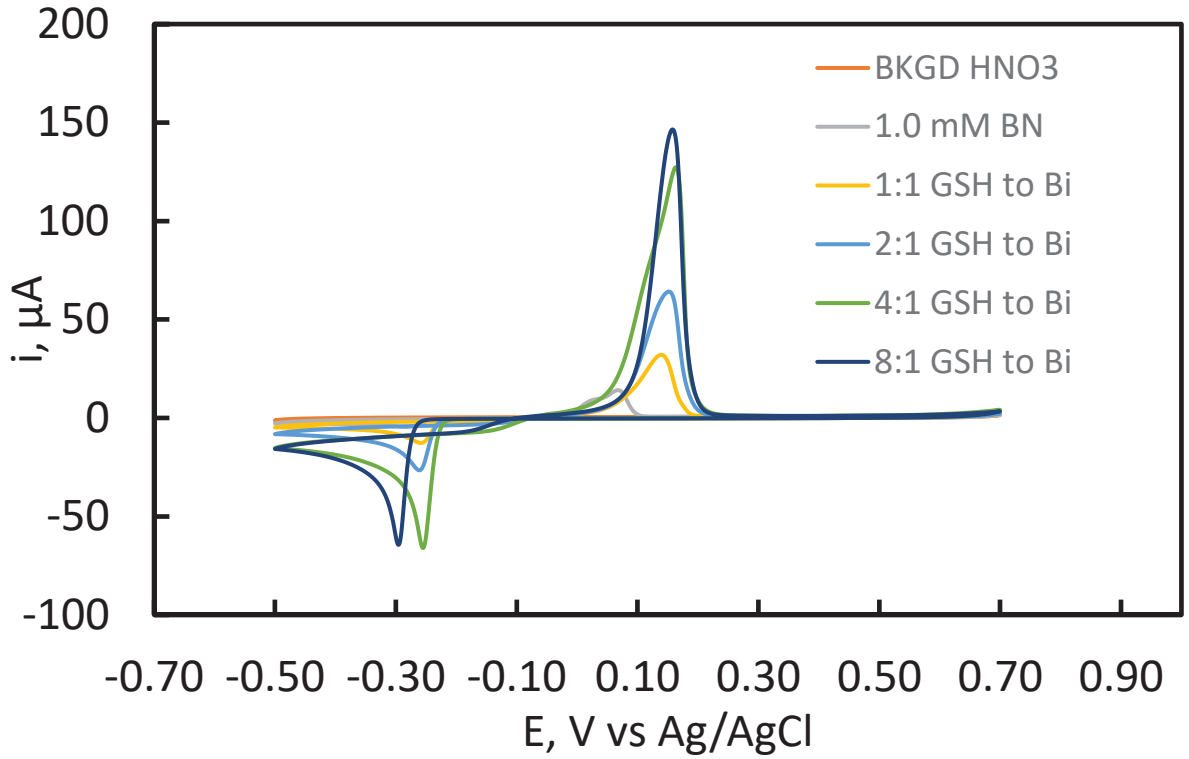

Figure 10. Cyclic voltammograms for 1.0 mM BN at glassy carbon in 0.10 M HNO_3, 100 mV/s, showing the effects of L-glutathione additions.

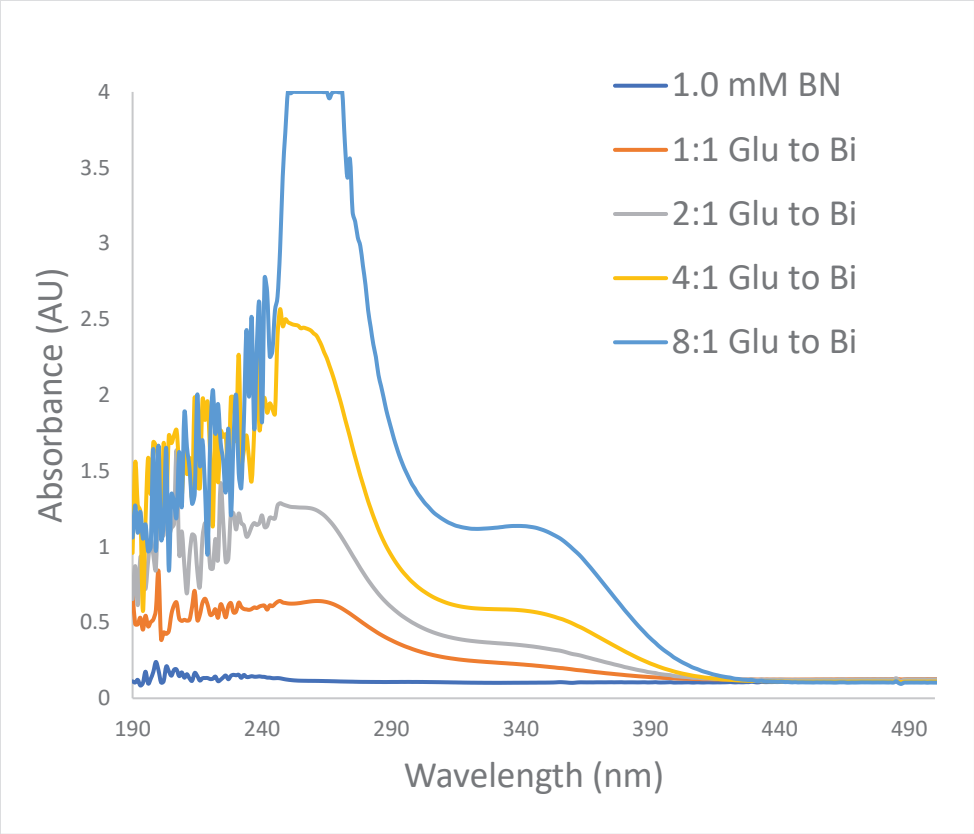

Figure 11. UV-Vis spectra of 1.0 mM BN in 0.10 M HNO_3, with incremental additions of L-glutathione. The path length was 1.00 cm.

Bismuth(III) nitrate in pH 3.0 in HNO_3, with L-cysteine additions

1.0 mM BN in pH 3.0 nitric acid showed greater solubility than 1.0 mM BN in pH 1.0 HCl as well as at pH 1.0 HNO_3. This is indicated by a larger stripping peak for the 1.0 mM BN solution at 170 µA rather than at 140 µA for the 1.0 mM BN solution in pH 1.0 HNO_3 (Figure 11 and 12). Subsequent additions of L-cysteine brought the bismuth further into solution, as shown with the increase in the max current, and an additional reduction potential shift for the 4:1 and 8:1 Cys to Bi ratio. By the 4:1 and 8:1 Cys to Bi ratios, the complex between Cys and Bi has fully formed, due to the slight change in reduction potential from -0.34 V to -0.41 V. These results are further supported by UV-Vis spectroscopy (Figure 13). Absorbance peaks at 350 nm for the 4:1 and 8:1 Cys to Bi ratios are present, which means that a bismuth-cysteine complex has formed beyond the 4:1 Cys to Bi point. At the 1:1 and 4:1 Cys to Bi ratios, a peak at 350 nm was not observed, meaning that the complex has not fully formed yet. These results parallel the ultimate reduction potential shift for the 4:1 and 8:1 ratio for the cyclic voltammograms. In this slightly less acidic

environment, complexation still happens, but requires an excess of ligands to drive the reaction towards the formation of the complex.

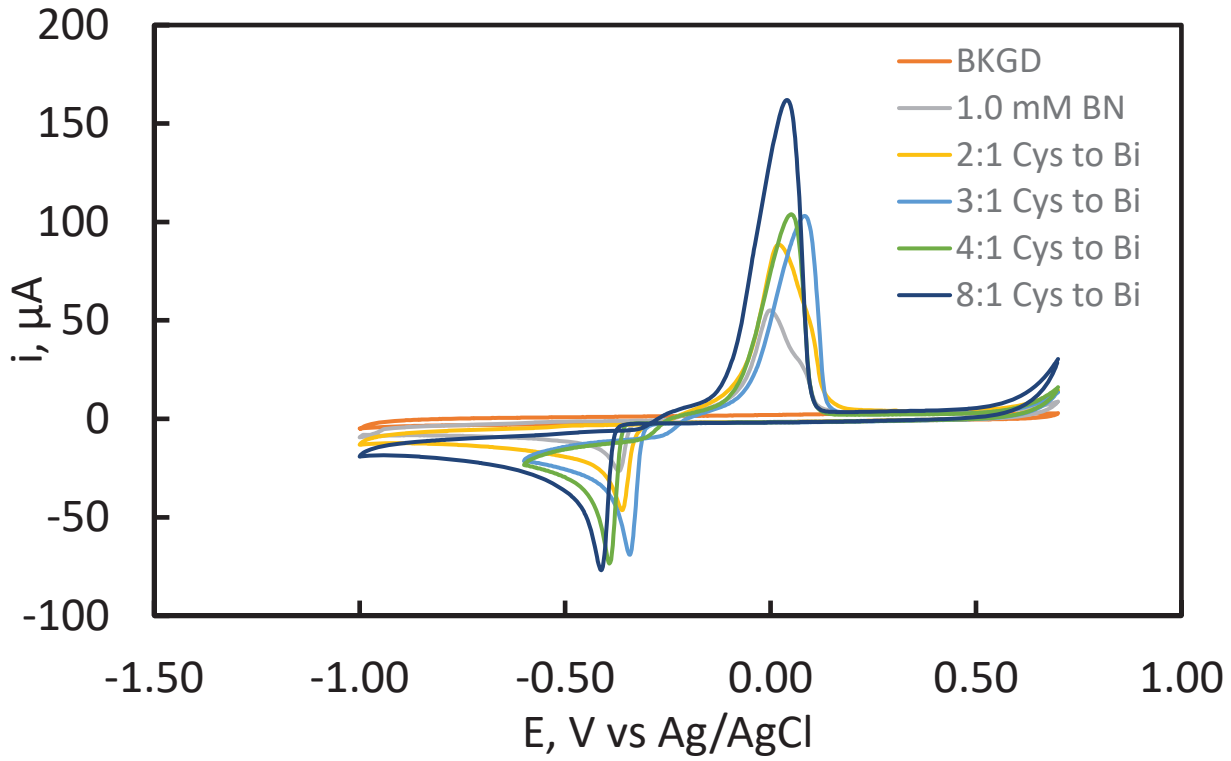

Figure 12. Cyclic voltammograms for 1.0 mM nominal BN at glassy carbon in 1.0 x 10^{-3} M HNO_3 (0.10 M ionic strength), 100 mV/s, showing the effects of L-cysteine additions.

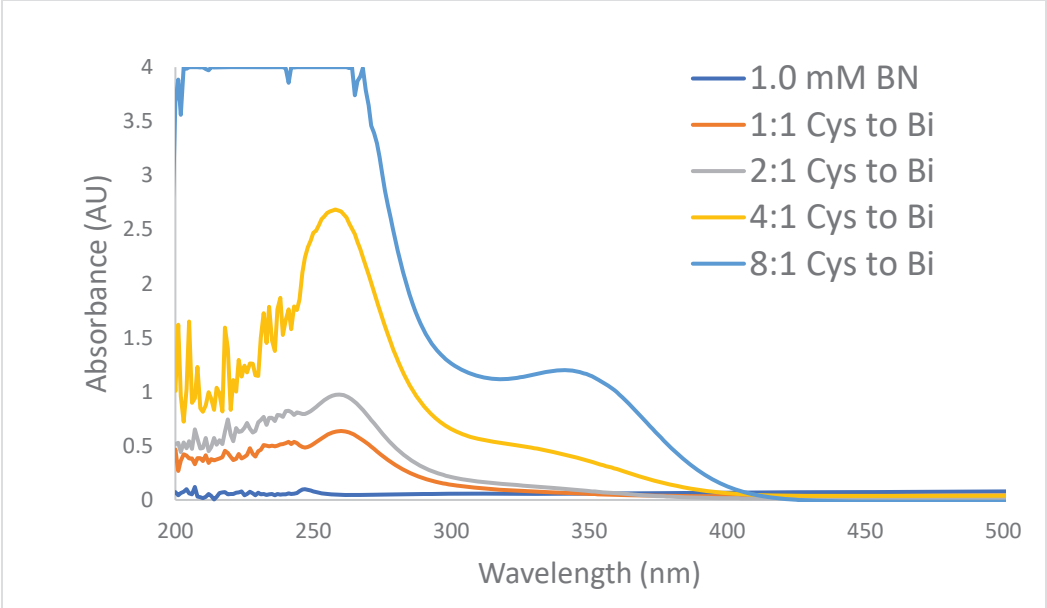

Figure 13. UV-Vis spectra of 1.0 mM BN in 1.0 x 10^{-3} M HNO_3 (0.1 M ionic strength), with incremental additions of L-cysteine. The path length was 1.00 cm.

Bismuth(III) nitrate (BN) in pH 3.0 in HCl, with L-cysteine additions

In an effort to compare the effect of pH and solvent on complexation, a nominal 1.0 mM BN solution was created in pH 3.0 HCl. From the UV-Vis spectra, it appears that Bi^{3+} in pH 3.0 HCl forms a complex more readily than at pH 3.0 nitric acid (Figures 13 and 14). This is due to the presence of a 350 nm peak for the 1:1 and 2:1 Cys to Bi sample in pH 3.0 HCl, whereas a 350 nm peak was not observed for the 1:1 and 2:1 Cys to Bis sample in pH 3.0 nitric acid. Additionally, the signal from the initial absorbance of 1.0 mM BN is much greater in pH 3.0 HCl than pH 3.0 nitric acid. Complexation by the chloride ion evidently causes BN to be much soluble in pH 3.0 HCl than in pH 3.0 HNO_3. However, the 1.0 mM BN solution in pH 3.0 HNO_3 was slightly less cloudy than the 1.0 mM BN solution in pH 3.0 HCl. While the UV-Vis spectra supports the formation of a complex between BN and Cys, a cyclic voltammogram must be obtained for the 1.0 mM BN in pH 3.0 HCl in order to support this conclusion.

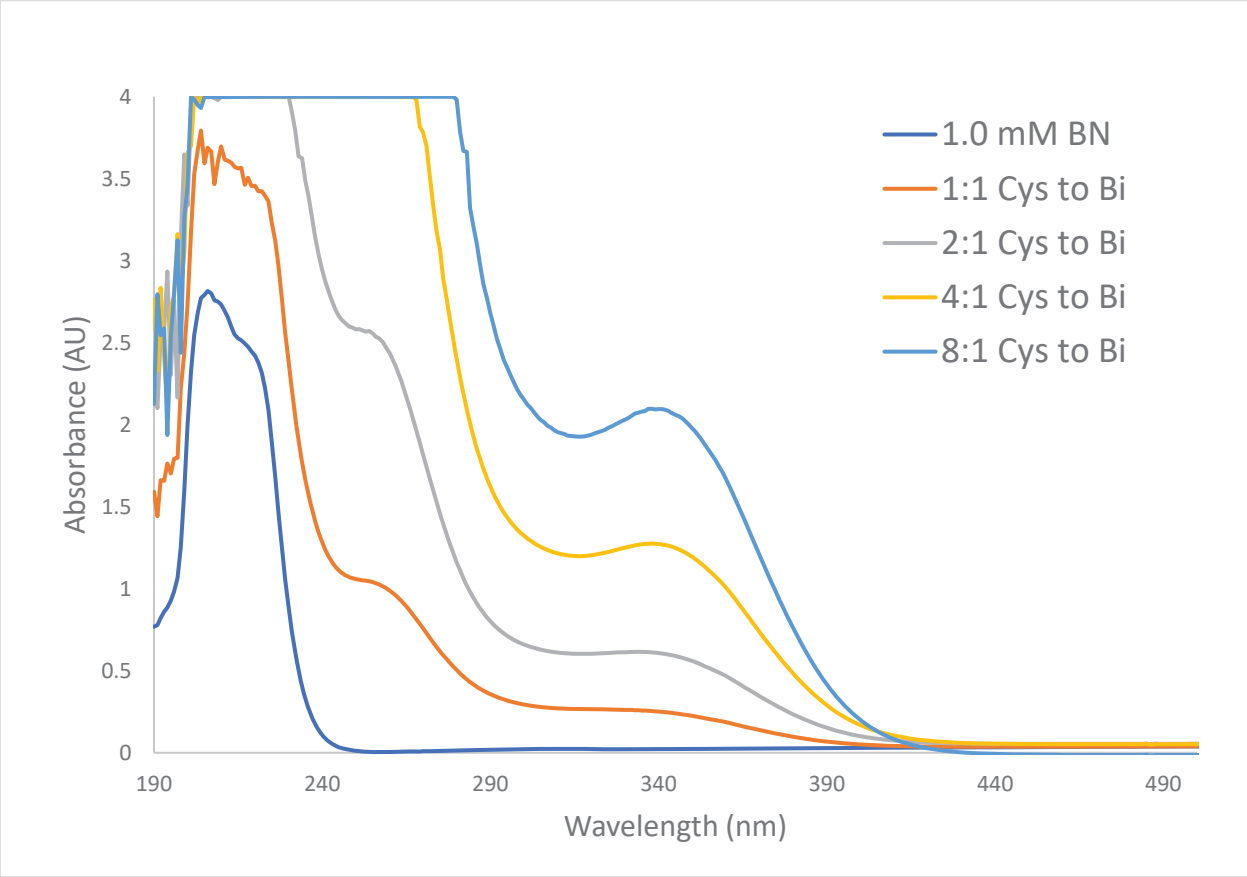

Figure 14. UV-Vis spectra of 1.0 mM BN in 1.0 x 10^{-3} M HCl (0.1 M ionic strength), with incremental additions of L-cysteine. The path length was 1.00 cm.

Bismuth(III) nitrate (BN) in pH 7.4 in MOPS, with L-cysteine additions

From a previous study performed by Cheek and Peña, BN was found to form a $Bi(Cys)_2$ complex with L-cysteine under physiological conditions, using cyclic voltammetry and UV-Vis spectroscopy (21). The earlier results were confirmed by repeating the experiment in the present study (Figure 15).

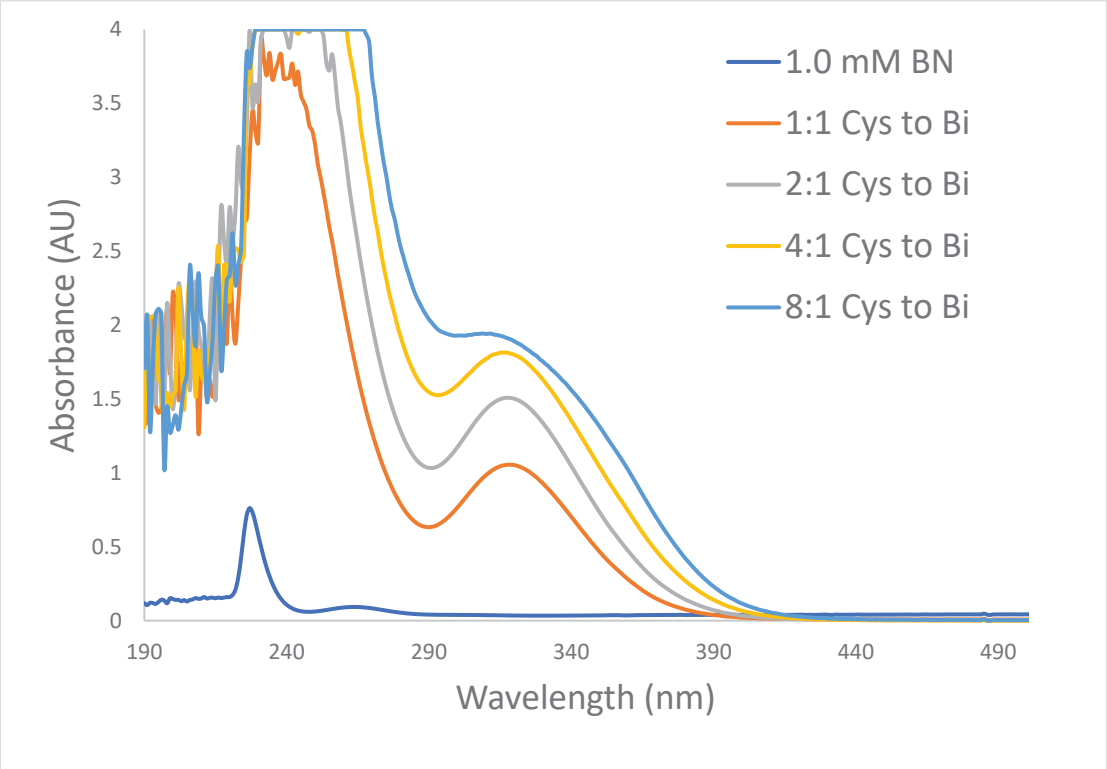

Figure 15. UV-Vis spectra of 1.0 mM BN in 0.10 M MOPS (buffered to pH 7.4), with incremental additions of L-cysteine. The path length was 1.00 cm.

Bismuth(III) nitrate in pH 7.4 in MOPS, with L-glutathione additions

At pH 7.4, the carboxyl group on L-glutathione is negatively charged, enhancing its ability to complex with Bi^{3+}. The results of the cyclic voltammogram confirm the complexation process. As higher ratios of GSH to Bi are added to the solution at pH 7.4, the maximum current increases, eventually capping at 72 μA for the peak stripping current for the 4:1 and 8:1 GSH to Bi ratios (Figure 16). Additionally, this information also confirms that the fully formed Bi-GSH complex occurred between the 2:1 and 4:1 GSH to Bi ratios. X-ray crystallography would be needed to confirm the structure of the complex and specify the exact ratio of GSH to Bi for the fully formed complex. UV-Vis spectroscopy of BN with L-glutathione in pH 7.4 MOPS also shows the characteristic complexation peak between bismuth and L-glutathione at 350 nm wavelength (Figure 17). However, the absorbance units were considered very low compared to other experiments in the same pH conditions that showed strong interactions between bismuth ions and these sulfur-containing biomolecules. After leaving the samples to stir overnight, UV-Vis spectroscopy was performed on the samples again, and this time, the absorbance values were much higher and the peaks were better defined (Figure 18). This presents a unique implication on the kinetics of complexation between the two ligands. Although L-glutathione was able to interact and complex with bismuth(III) ions, the rate at which complexation occurs, occurred on a slower timescale than its L-cysteine counterpart. This may be explained by steric hinderances, since L-glutathione is a larger molecule than is L-cysteine, and it might need more time to orient itself in a position for the sulfur ligand to interact with the bismuth ion.

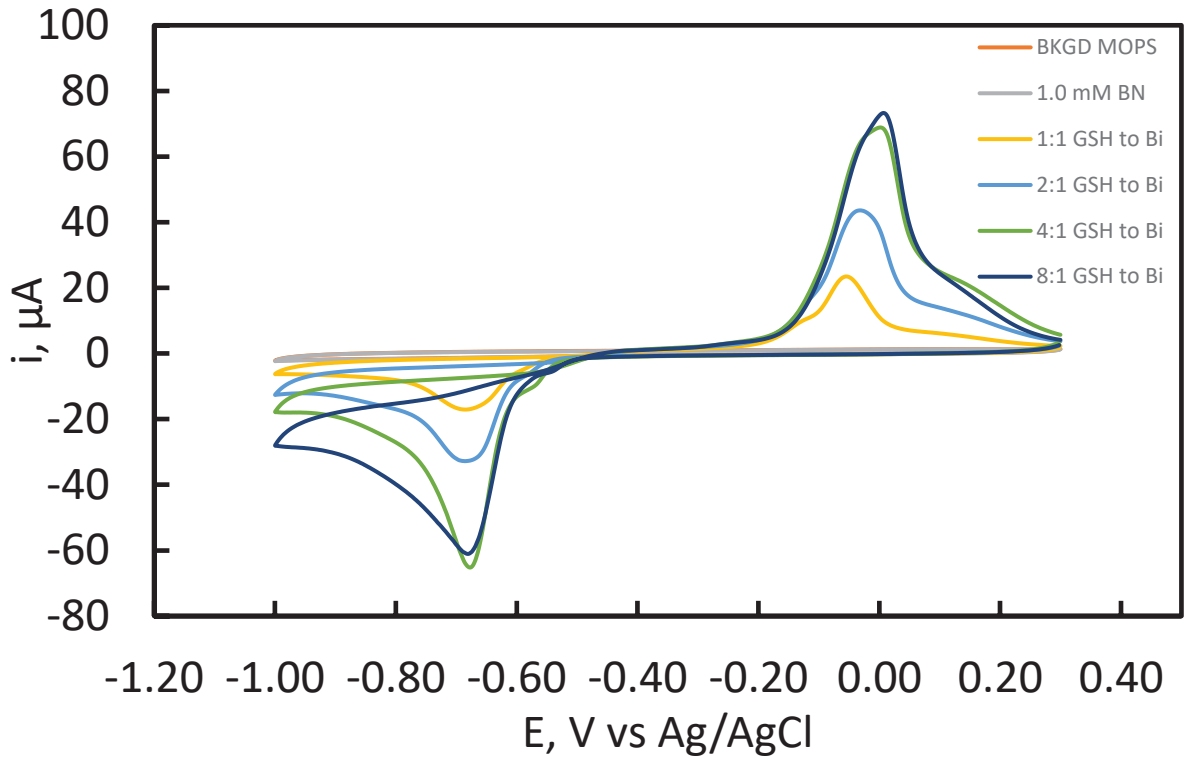

Figure 16. Cyclic voltammograms for 1.0 mM BN at glassy carbon in 0.10 M MOPS (buffered at pH 7.4), 100 mV/s, showing the effects of L-glutathione additions.

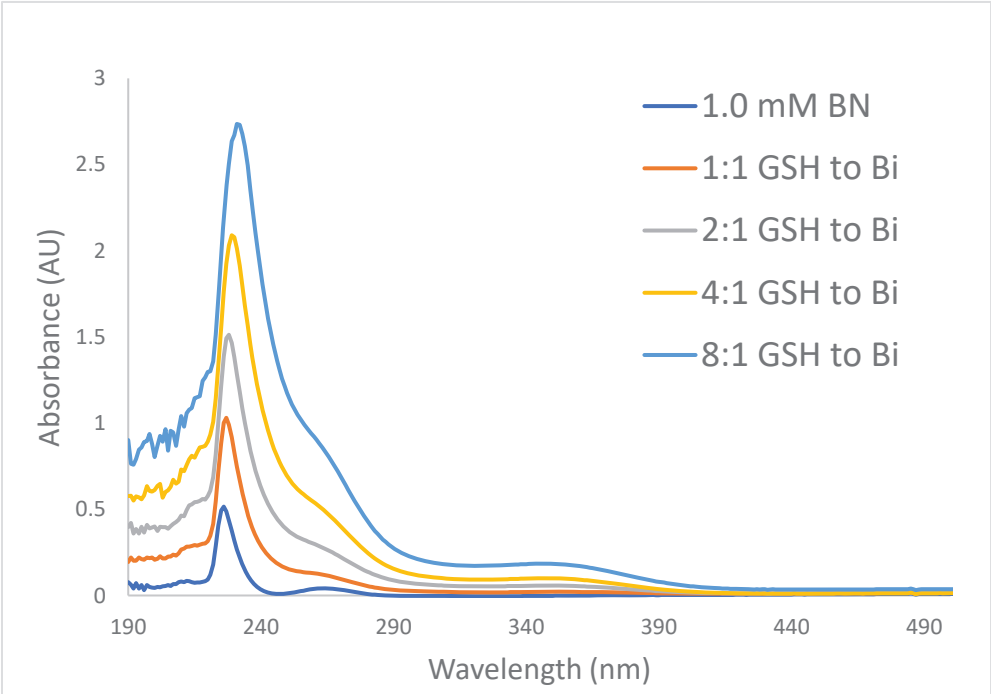

Figure 17. UV-Vis spectra of 1.0 mM BN in 0.10 M MOPS (buffered to pH 7.4), with incremental additions of L-glutathione. The path length was 1.00 cm.

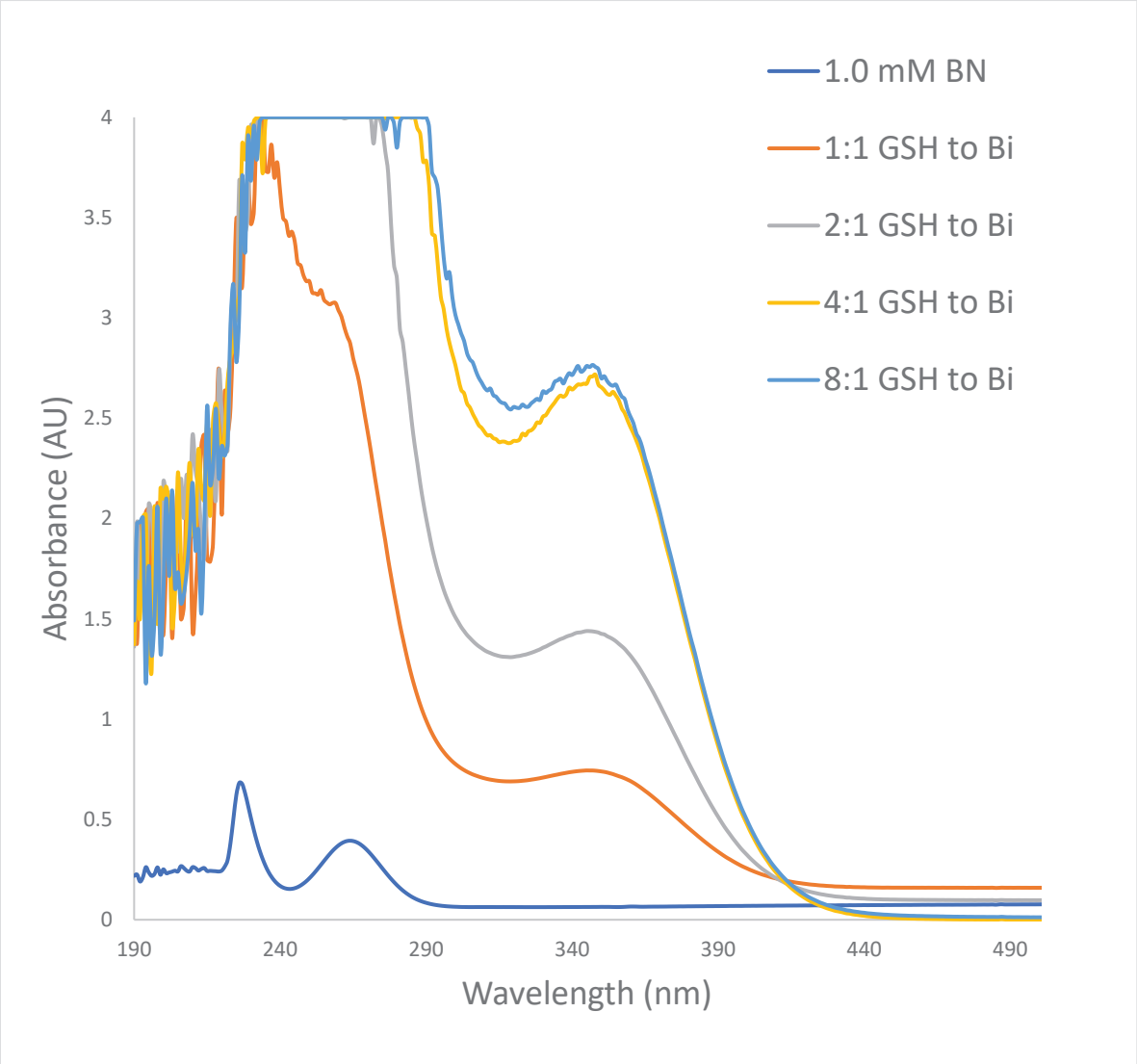

Figure 18. UV-Vis spectra of 1.0 mM BN in 0.10 M MOPS (buffered to pH 7.4), with incremental additions of L-glutathione. The path length was 1.00 cm. Results were obtained after solutions were left stirring overnight for 24 hours.

Bismuth(III) salicylate (BSS) in pH 1.0 HNO_3 with L-cysteine additions

BSS was found to be soluble at the 1.0 mM level in pH 1.0 HNO_3. BSS in pH 1.0 nitric acid showed similar stripping profiles at all ratios of L-cysteine to bismuth; however, the reduction potential was found to shift slightly toward more negative values as more L-cysteine was added (Figure 19). This observation demonstrates that Bi-Cys complexes are forming due to an application of Le Châtelier's principle and the metal complex term of the Nernst equation (Equation 4). UV-Vis spectroscopy shows that gradual increases of L-cysteine concentration

slightly increased the absorbance shoulder at 350 nm wavelength, signaling increased complexation formation (Figure 20). Large peaks at 300 nm indicate the absorbance of the salicylate ligand, which remain even as L-cysteine concentration increases. This along with rather small changes in the voltammetric response, implies that complexation of bismuth salicylate is not particularly extensive in pH 1.0 nitric acid.

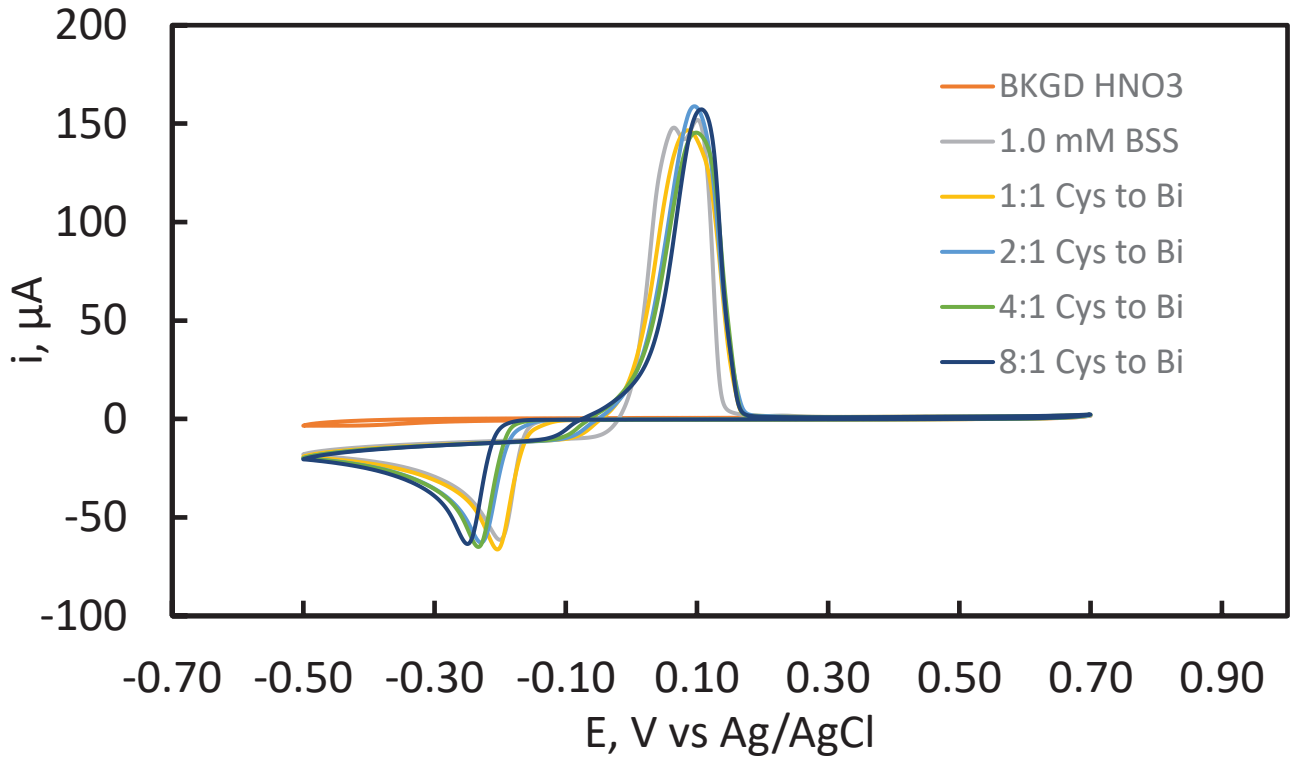

Figure 19. Cyclic voltammograms for 1.0 mM BSS at glassy carbon in 0.10 M HNO_3, 100 mV/s, showing the effects of L-cysteine additions.

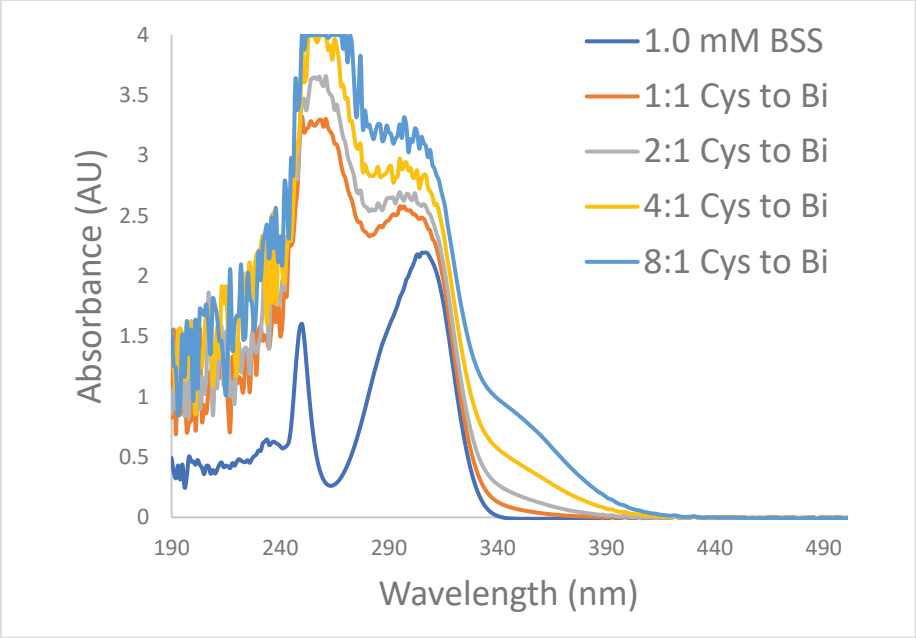

Figure 20. UV-Vis spectra of 1.0 mM BSS in 0.10 M HNO_3, with incremental additions of L-cysteine. The path length was 1.00 cm.

Bismuth(III) salicylate (BSS) in pH 1.0 HNO_3 with L-glutathione additions

Similar to the case for BSS with L-cysteine additions in pH 1.0 nitric acid (Figures 19 and 20), BSS with L-glutathione (GSH) additions in the same medium resulted in similar voltammetric characteristics (Figures 19 and 21). Both are marked by a maximum stripping current of around 150 μA, which is indicative of the same plating and stripping behavior. Both have relatively high peak currents, indicating that BSS and its GSH complexes are soluble at 1.0 mM. Furthermore, the reduction potential has generally shifted toward the more negative values with subsequent additions of GSH. As the GSH complexes are forming, the reduction potential shifts to more negative values. In Figure 21, the reduction potential shifts stop at -0.25 V at the 4:1 and 8:1 GSH to Bi ratio. This means that between the 4:1 and 8:1 GSH to Bi ratio, there were enough GSH molecules to fully form the complex. UV-Vis spectra further supports the formation of the Bi-GSH complex due to the presence of the 340 nm wavelength peak (Figure 22). It should be noted that the absorbance for the 340 nm peak is roughly twice that seen in Figure 20, indicating that the extent of complexation is greater for GSH than for L-cysteine. In either case, the continuing peak potential shifts and absorbance increases at 340 nm do not imply that 8:1 ligand:Bi complexes are formed, but they simply reflect the necessary high concentrations of the ligands required to drive the metal : ligand interaction to some extent. The high concentration of protons (0.10 M) assures the complete protonation of the ligand carboxylate functional groups, thereby limiting their ability to form complexes with Bi^{3+}.

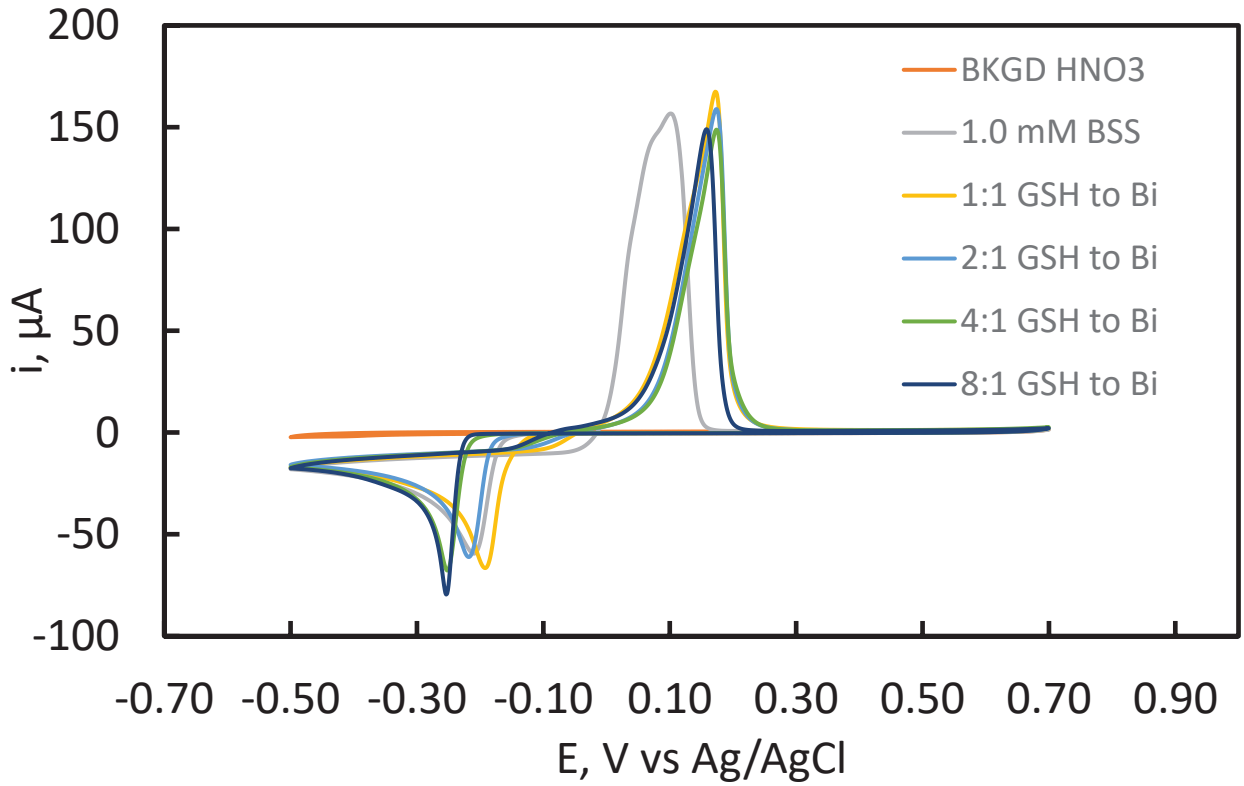

Figure 21. Cyclic voltammograms for 1.0 mM BSS at glassy carbon in 0.10 M HNO_3, 100 mV/s, showing the effects of L-glutathione additions.

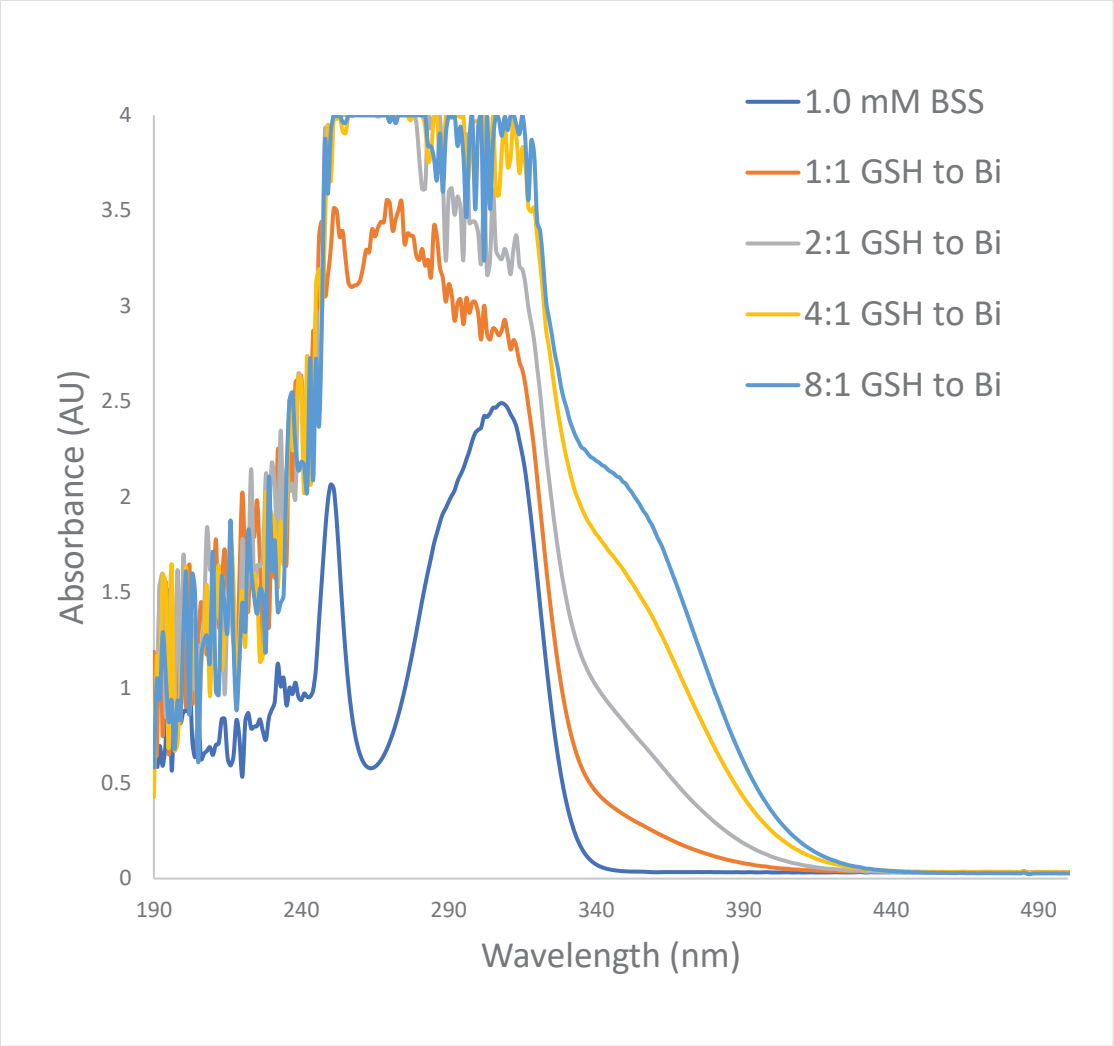

Figure 22. UV-Vis spectra of 1.0 mM BSS in 0.10 M HNO_3, with incremental additions of L-glutathione. The path length was 1.00 cm. The samples were stirred overnight.

Bismuth(III) salicylate (BSS) in pH 1.0 HCl, with L-cysteine additions

A 1.0 mM BSS solution was created in pH 1.0 HCl to see what effect a bidentate ligand and the chloride ligand would have on L-cysteine's ability to complex with Bi^{3+}. The cyclic voltammogram showed very weak stripping and reduction signals at all ratios up to 4:1 Cys to Bi, confirming the poor solubility of BSS in 0.10 M hydrochloric acid (Figure 23). The 8:1 Cys to Bi ratio showed a larger spike in the maximum stripping current; however, compared to the expected values from the nitric acid solution, the 0.10 M hydrochloric acid solutions still yielded low current. These weak signals are explained by the weak interactions between L-cysteine and the bismuth ions at this particular pH and medium, evidently due to the formation of chloride complexes with bismuth. From the UV-Vis spectra, a sharp peak at 290-300 nm can be observed (Figure 24). This peak originates from the salicylate ligand, which has its own unique signal at that range. The 1:1 and 2:1 Cys to Bi ratios do not manifest a peak at 350 nm, implying that at that concentration of L-cysteine, a complex cannot form due to various reasons such as the chloride effect or the high concentration of protons. At the 4:1 and 8:1 Cys to Bi ratio, a very slight shoulder can be seen at 350 nm, yet there is a persistent absorbance at wavelengths beyond 400 nm, due to scattering by solid in the light path. At all ratios of Cys to Bi, the solution was always cloudy, indicating that the chloride ions, and to some extent, the salicylate ligand, have a stronger affinity for the bismuth ions than cysteine at a pH of 1.0 in HCl.

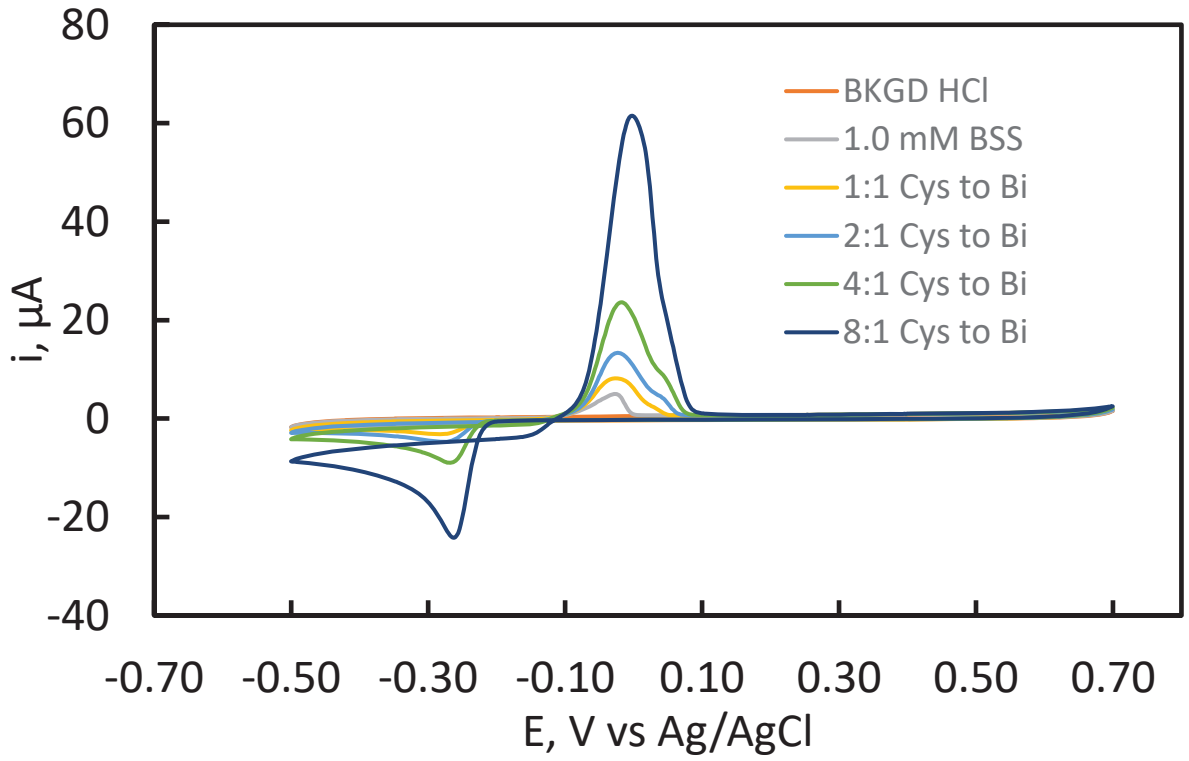

Figure 23. Cyclic voltammograms for 1.0 mM BSS at glassy carbon in 0.10 M HCl, 100 mV/s, showing the effects of L-cysteine additions.

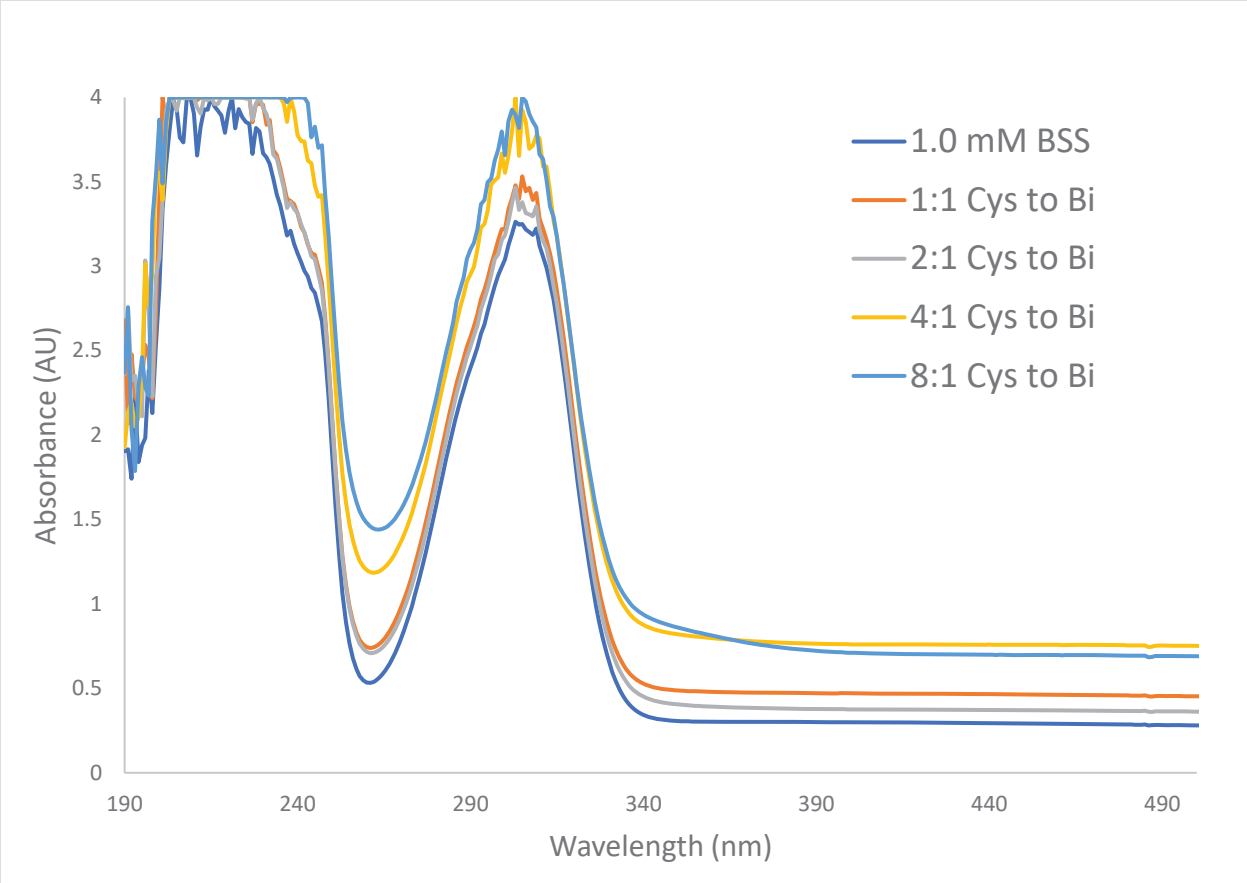

Figure 24. UV-Vis spectra of 1.0 mM BSS in 0.10 M HCl, with incremental additions of L-cysteine. The path length was 1.00 cm.

Bismuth(III) salicylate (BSS) in pH 1.0 HCl, with L-glutathione additions

In contrast to L-cysteine, L-glutathione additions were able to elicit a stronger electrochemical signal at the same pH and in the same solvent. Magnitudes of the peak reduction current and the stripping current were nearly double that of the signals from L-cysteine additions to BSS (Figures 23 and 25). In addition, the presence of two stripping peaks indicate the involvement of chloride in the complexation process, as noted earlier. The results imply that L-glutathione is a stronger ligand than L-cysteine by being able to complex and bring more bismuth ions into solution, although the interaction is still rather weak. The UV-Vis spectra do not clarify the interactions between the GSH ligands and the bismuth ions due to a high level of scattering at the base line (Figure 26). The solution never became clear during the course of this experiment. This conceals some of the complexation peaks that otherwise would point to the relative affinities of GSH for bismuth ions. To combat this issue, more time would be needed to allow the suspended particles in the solution to settle. The results of this experiment also demonstrates the kinetically slow complexation process between BSS and GSH.

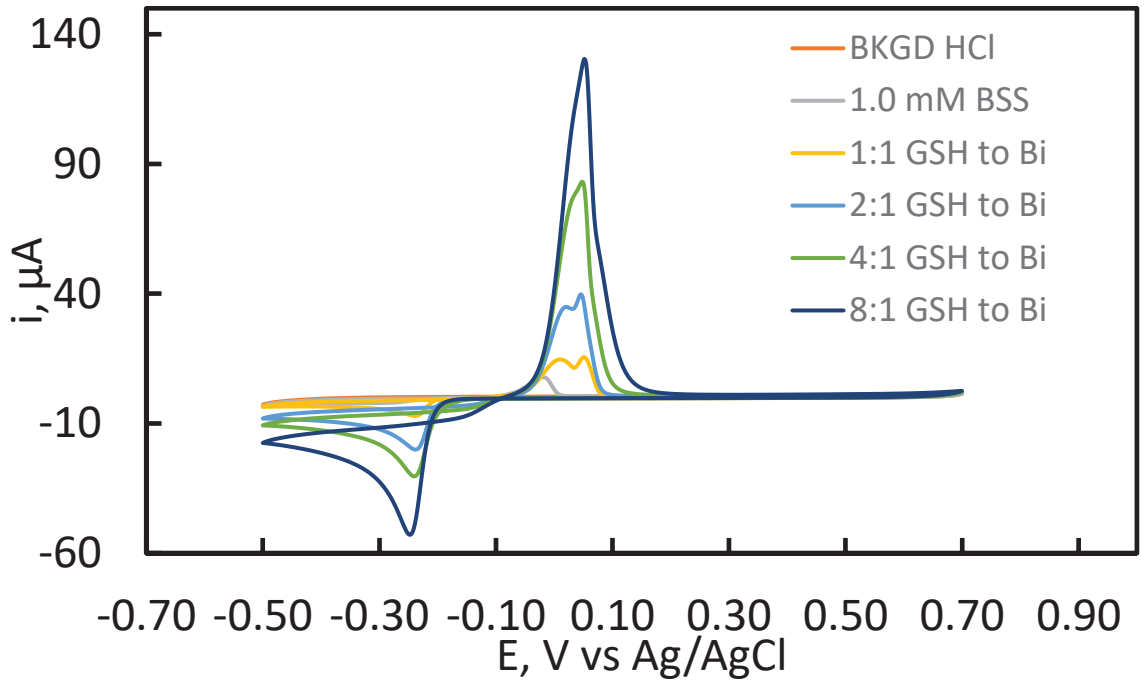

Figure 25. Cyclic voltammograms for 1.0 mM BSS at glassy carbon in 0.10 M HCl, 100 mV/s, showing the effects of L-glutathione additions.

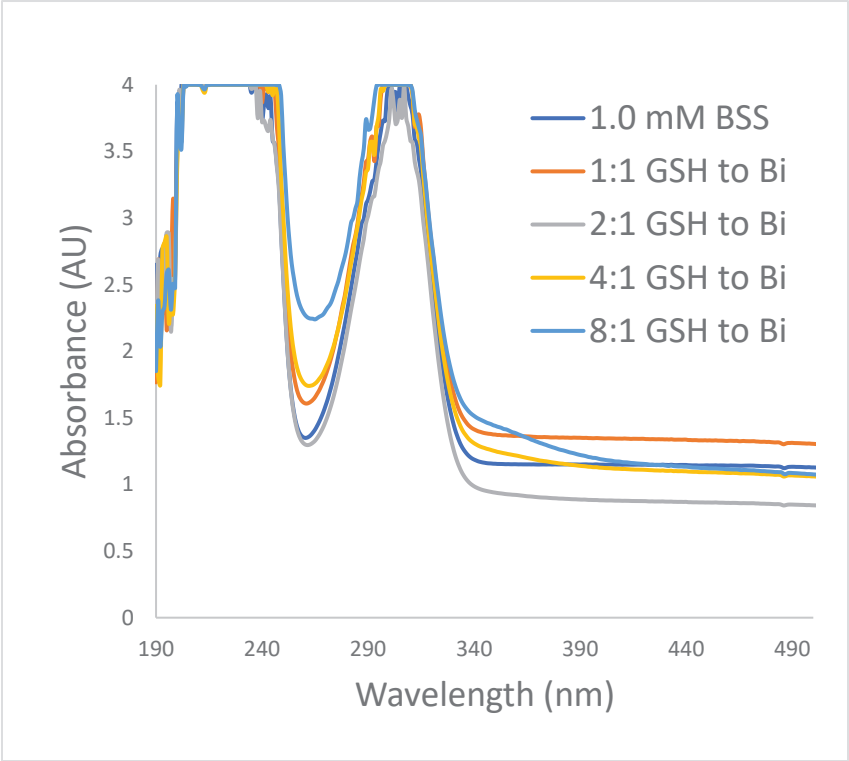

Figure 26. UV-Vis spectra of 1.0 mM BSS in 0.10 M HCl, with incremental additions of L-glutathione. The path length was 1.00 cm.

Bismuth(III) salicylate (BSS) in pH 3.0 HCl, with L-cysteine additions

A one-hundred-fold dilution of the 0.10 M HCl allowed the nominal 1.0 mM BSS solution to interact with L-cysteine. In the cyclic voltammogram, the bismuth is initially not very soluble in HCl (Figure 27). However, subsequent additions of L-cysteine brought the bismuth into solution gradually, as indicated by the increasing peak current. However, the bismuth-cysteine complex, at whatever ratio, did not fully form until the 8:1 Cys to Bi ratio as seen by the slight negative potential shift. The gradual formation of the bismuth-cysteine complex is also supported by the cyclic voltammogram (Figure 28). At the 1:1 Cys to Bi ratio, a 350 nm peak was not observed, but starting at 2:1 Cys to Bi, a slight peak can be observed. At the 4:1 sample, the peak is more prominent, with the 8:1 sample culminating to the maximum signal and visually becoming clear and colorless, indicating that complexation is essentially complete, as also seen in the cyclic voltammogram (Figures 27 and 28). From these results, L-cysteine has a higher affinity for Bi(III) once the pH value has increased, indicating that at very low pH ranges the protonation state for L-cysteine hinders any favorable interactions with Bi(III).

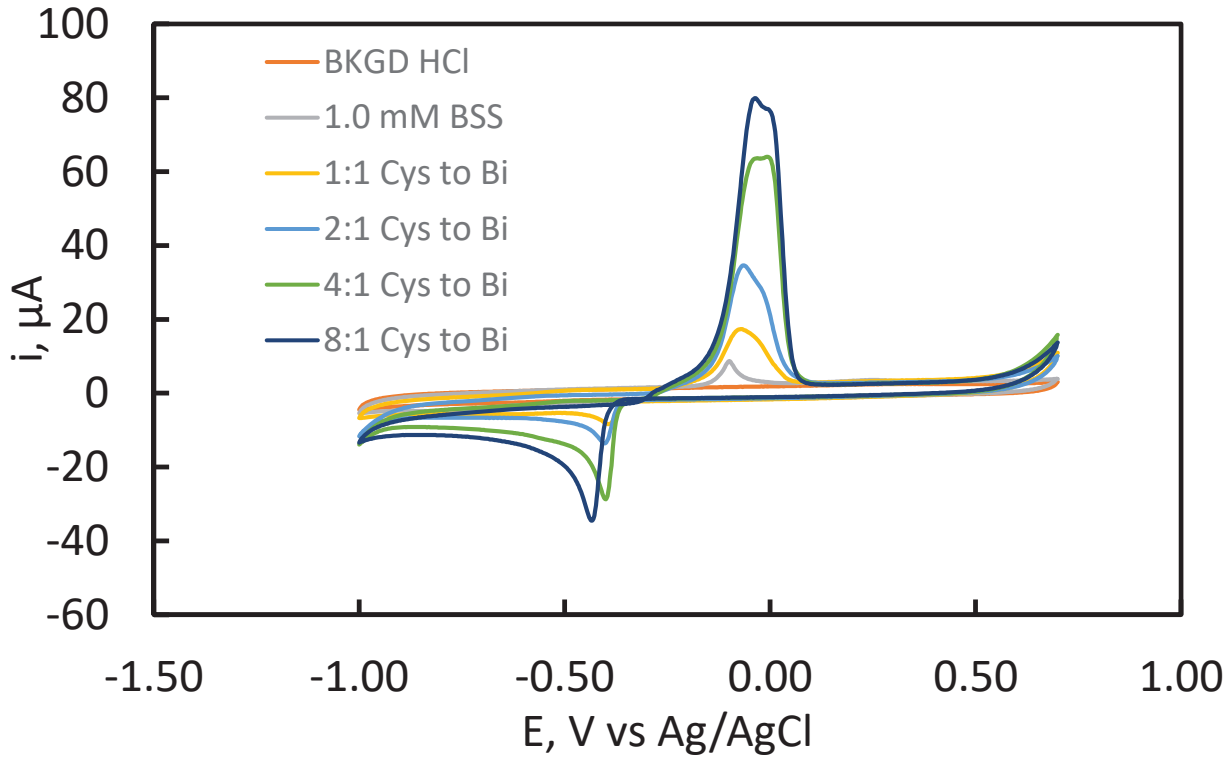

Figure 27. Cyclic voltammograms for 1.0 mM BSS at glassy carbon in 1.0 x 10^{-3} M HCl (0.1 M ionic strength), 100 mV/s, showing the effects of L-cysteine additions.

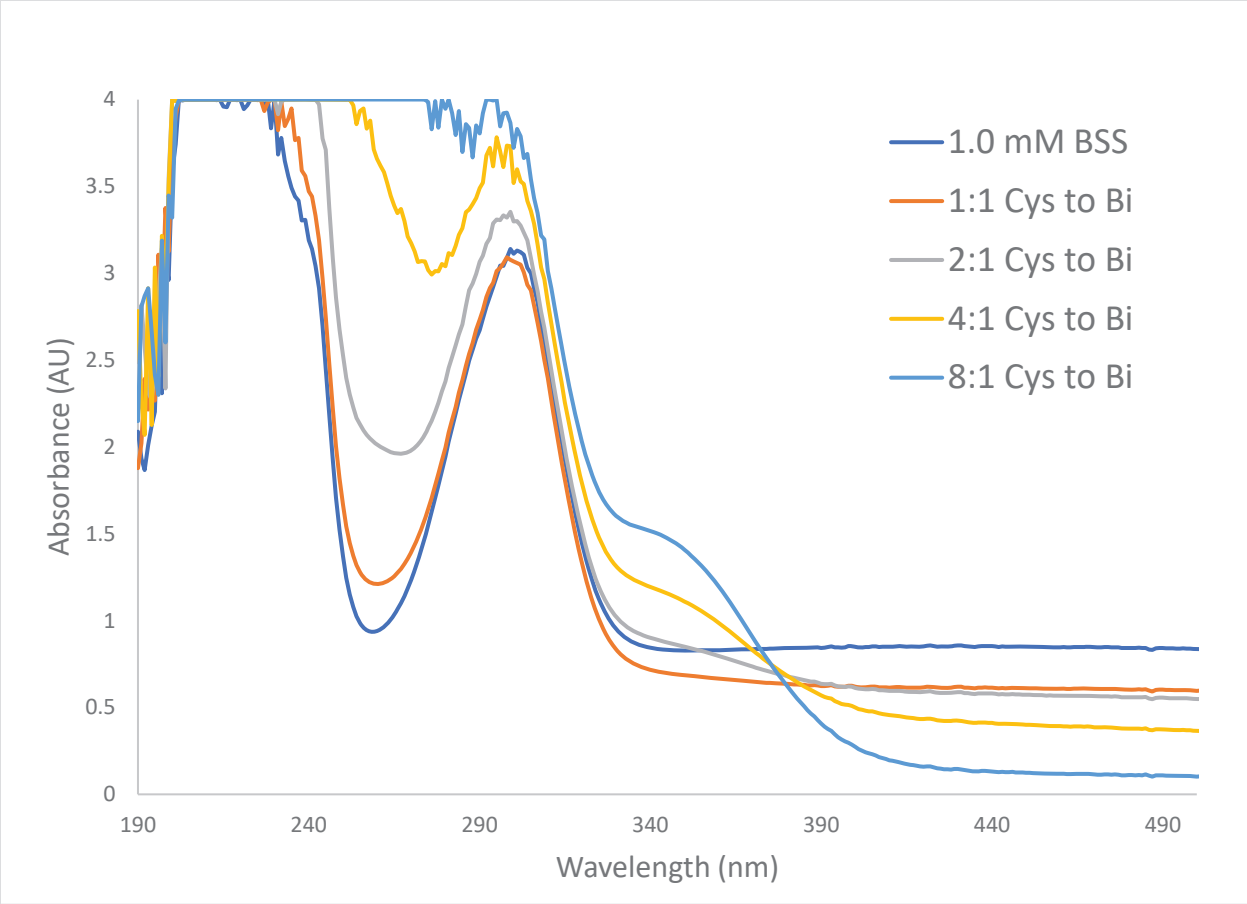

Figure 28. UV-Vis spectra of 1.0 mM BSS in 1.0 x 10^{-3} M HCl (0.1 M ionic strength), with incremental additions of L-cysteine. The path length was 1.00 cm.

Bismuth(III) salicylate (BSS) in pH 7.40 MOPS, with L-cysteine additions

1.0 mM BSS was created in pH 7.40 MOPS buffer to mimic general physiological conditions. Compared to experiments at lower pH values, experiments at pH 7.40 in MOPS resulted in greater potential shifts and greater peak currents (Figures 29 and 30). The 1:1 Cys to Bi ratio gave a relatively narrow reduction peak at -0.62 V. The symmetry of the peak implies that the complex formed between L-cysteine and bismuth is surface bound to the glassy carbon electrode. The physical meaning of this peak is that the complex is not dissolved in the solution, leading to a higher, more symmetrical, current response. In addition, the stripping potential is more positive than the other ratios, and the charge for the stripping process is similar to that for the initial reduction. This suggests that the Bi(III) has a harder time being complexed by L-cysteine due to the lower concentration of ligands willing to complex. After the 4:1 Cys to Bi ratio, the sheer excess of cysteine concentration allows for more extensive interactions between Bi(III) and L-

cysteine. The UV-Vis spectra support the findings from the cyclic voltammogram – at every ratio of L-cysteine to bismuth, a peak can be observed at 350 nm. However, initially, the cell contents were cloudy and did not become clear until the 2:1 Cys to Bi addition. Because the peak absorbance does not increase much during these additions, it can be concluded that the complex is still forming at the 8:1 Cys to Bi ratio. Overall, the pH environment creates a favorable protonation state for L-cysteine to complex with Bi(III).

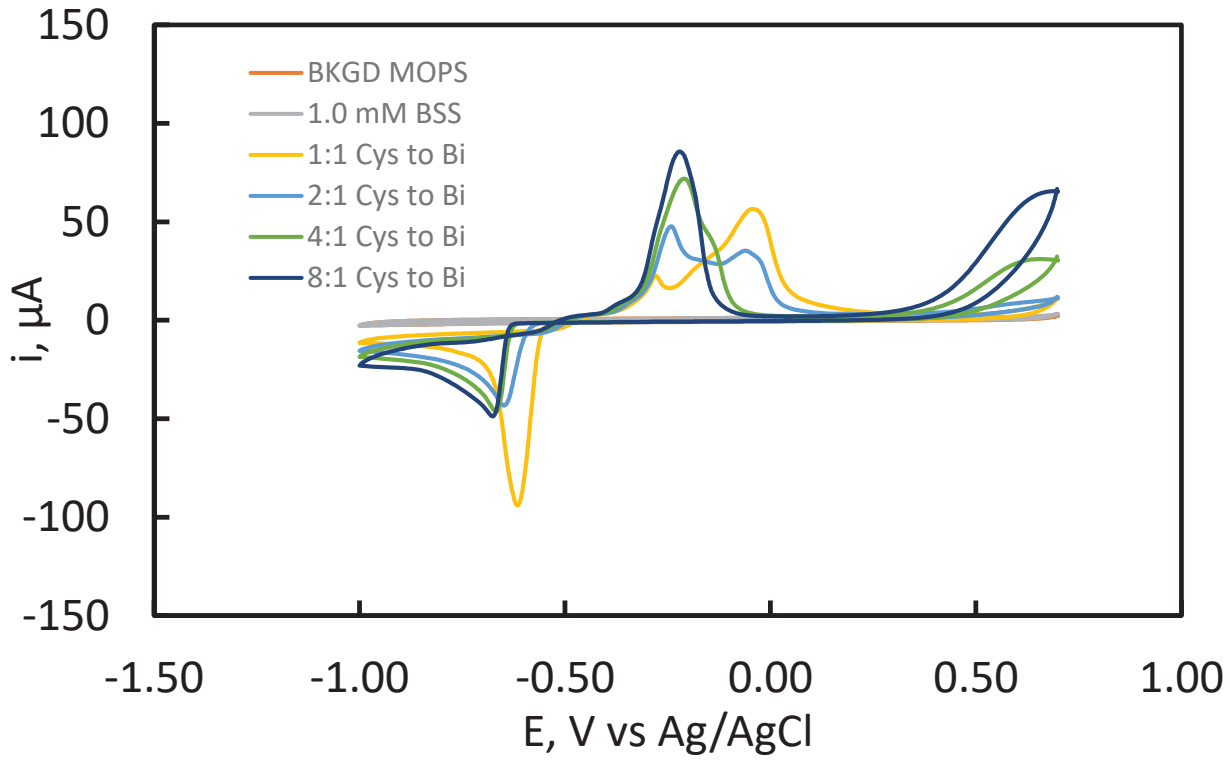

Figure 29. Cyclic voltammograms for 1.0 mM BSS at glassy carbon in pH 7.40 MOPS buffer, 100 mV/s, showing the effects of L-cysteine additions.

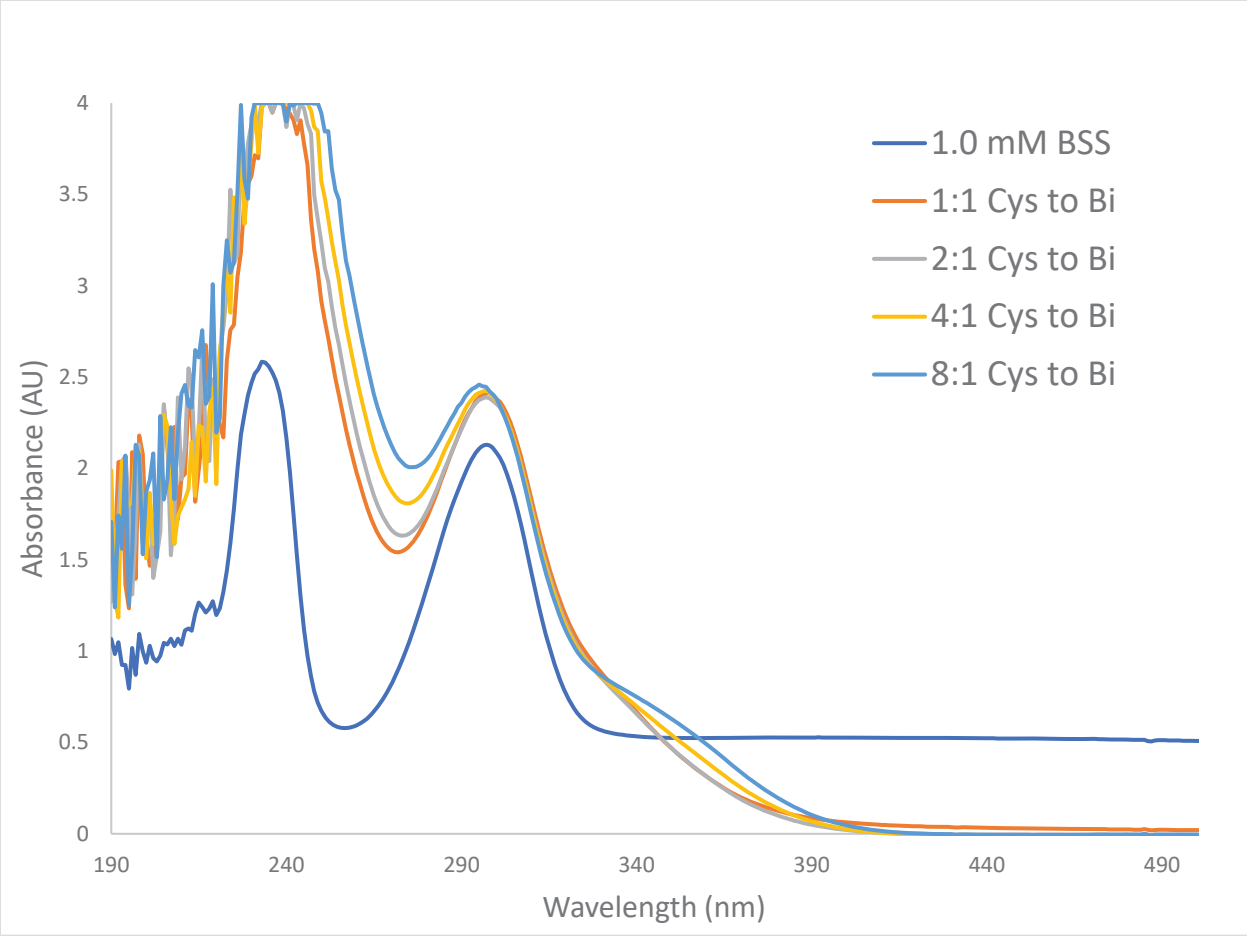

Figure 30. UV-Vis spectra of 1.0 mM BSS in pH 7.40 MOPS buffer, with incremental additions of L-cysteine. The path length was 1.00 cm.

Bismuth(III) salicylate (BSS) in pH 7.40 MOPS, with L-glutathione additions

BSS in pH 7.40 MOPS, upon the addition of L-glutathione, exhibited electrochemical signal changes from the initial nominal 1.0 mM BSS solution. Specifically, additions of GSH were met with increases to the peak current (Figure 31). After the 2:1 GSH to Bi ratio, the reduction peak current remained constant with the solution becoming clear, indicating no further changes to the solution. Likely, this means that the Bi-GSH complex has fully formed upon the addition of two molar equivalents of GSH. This detail gives insight on the ratio of GSH to Bi for a fully formed complex. The UV-Vis spectrum supports this observation as well, with the absorbance value for the complexation peak at 350 nm wavelength hitting a maximum at around 1.1 AU after the 2:1 GSH to Bi ratio (Figure 32). Similar behavior was found for the interaction between bismuth nitrate and L-cysteine in pH 7.40 MOPS buffer (21). Nevertheless, X-ray crystallography can be conducted to confirm the structure of the complex. The lower protonation state for L-cysteine at pH 7.40, compared to that at lower pH values, accounts for the complete formation of the complex at the 2:1 GSH to Bi ratio.

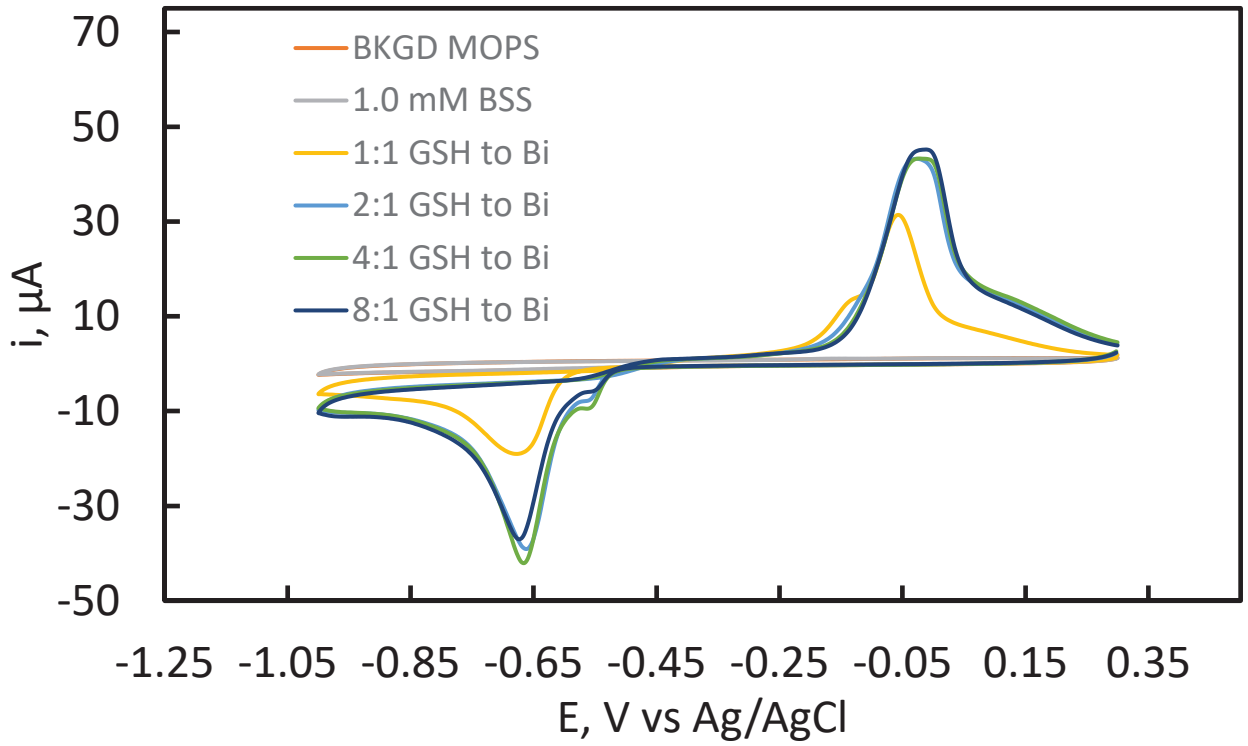

Figure 31. Cyclic voltammograms for 1.0 mM BSS at glassy carbon in pH 7.40 MOPS buffer, 100 mV/s, showing the effects of L-glutathione additions.

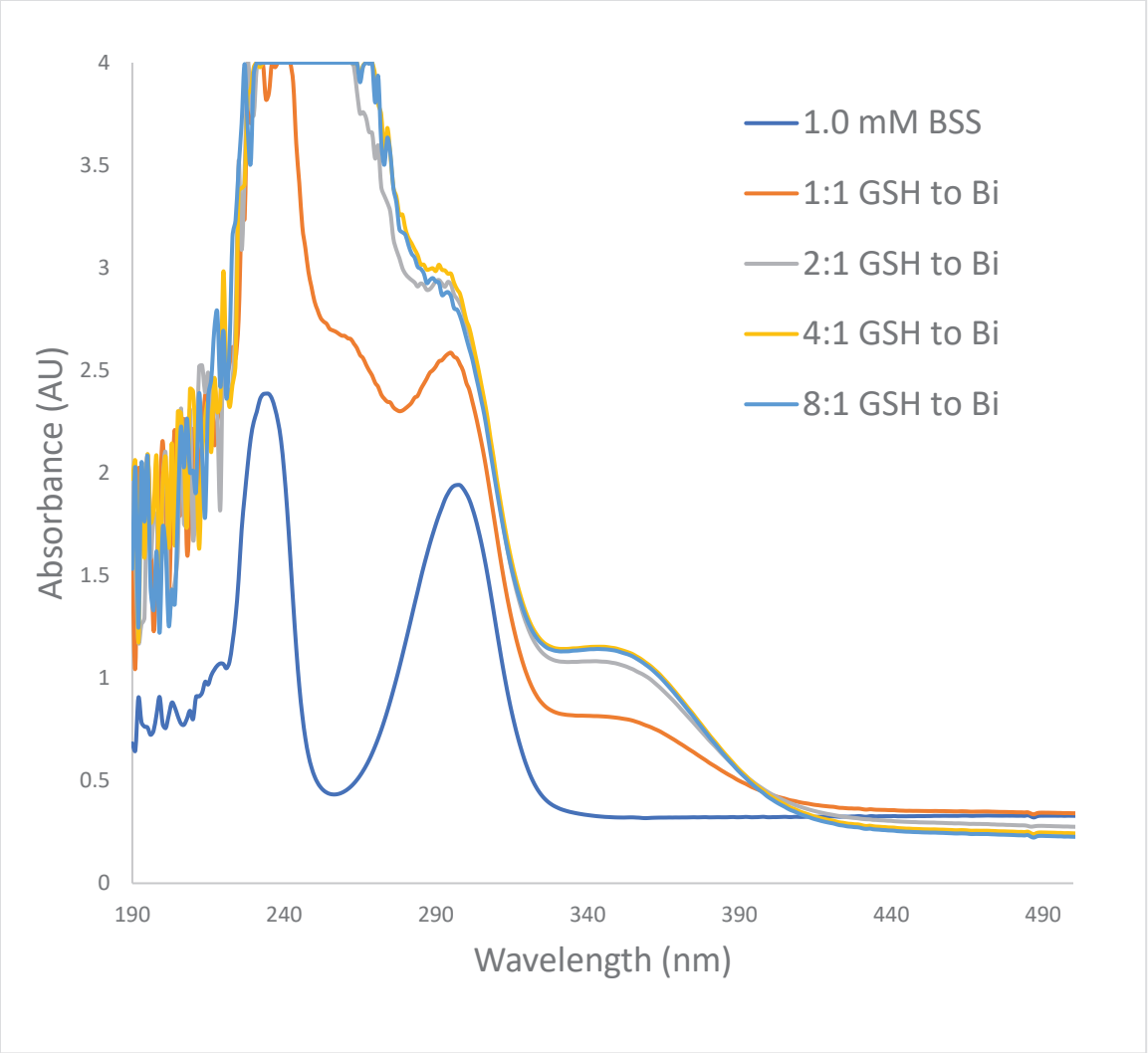

Figure 32. UV-Vis spectra of 1.0 mM BSS in pH 7.40 MOPS buffer, with incremental additions of L-glutathione. The path length was 1.00 cm.

Bismuth(III) citrate (BC) in pH 1.0 HCl, with L-cysteine additions

At pH 1.0 in HCl, BC undergoes a considerable reduction peak potential shift from -0.15 V to -0.26 V upon initial addition of L-cysteine, followed by only slight further negative shifts upon further additions to the 6:1 Cys to Bi point (Figure 33). The UV-Vis spectra do not indicate that the complex that was formed is necessarily a complex between L-cysteine and bismuth (Figure 34). This is supported by the visual inspection of the cell being cloudy at all ratios of Cys to Bi. Although a weak absorbance peak can be seen for all ratios of cysteine to bismuth, the peak does not fall in the 350 nm range. In addition, comparison of the UV spectra of BC in pH 1.00 HCl and HNO_3 shows that the 260 nm band due to complexation of bismuth with citrate in pH 1.00 HNO_3 (Figure 35) is absent at pH 1.00 HCl (Figure 33), implying that bismuth is complexed by chloride

ion in pH 1.00 HCl before addition of L-cysteine. The lack of a well-defined band at 350 nm implies that L-cysteine does not form the same complex as observed in other cases, although the voltammetric peak shifts support some role of L-cysteine as a ligand. This indicates that a mixed complex between the chloride ions and the L-cysteine ligands may be present in the solution. Finally, the 10:1 Cys to Bi sample resulted in a spike in the reduction peak current. This indicates that at that point, the overwhelming concentration of L-cysteine has brought most of the bismuth into solution. Overall, L-cysteine does not seem to complex very well with BC in pH 1.0 HCl.

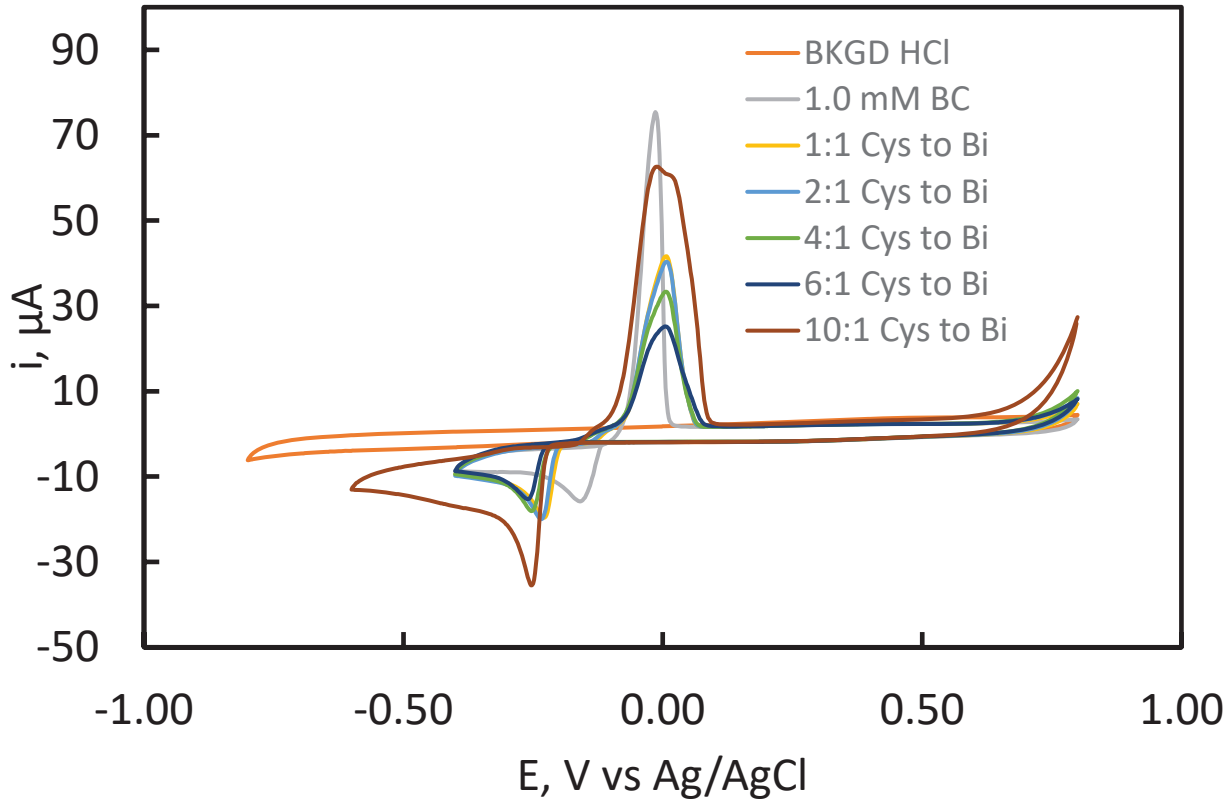

Figure 33. Cyclic voltammograms for 1.0 mM BC at glassy carbon in 0.10 M HCl, 100 mV/s, showing the effects of L-cysteine additions.

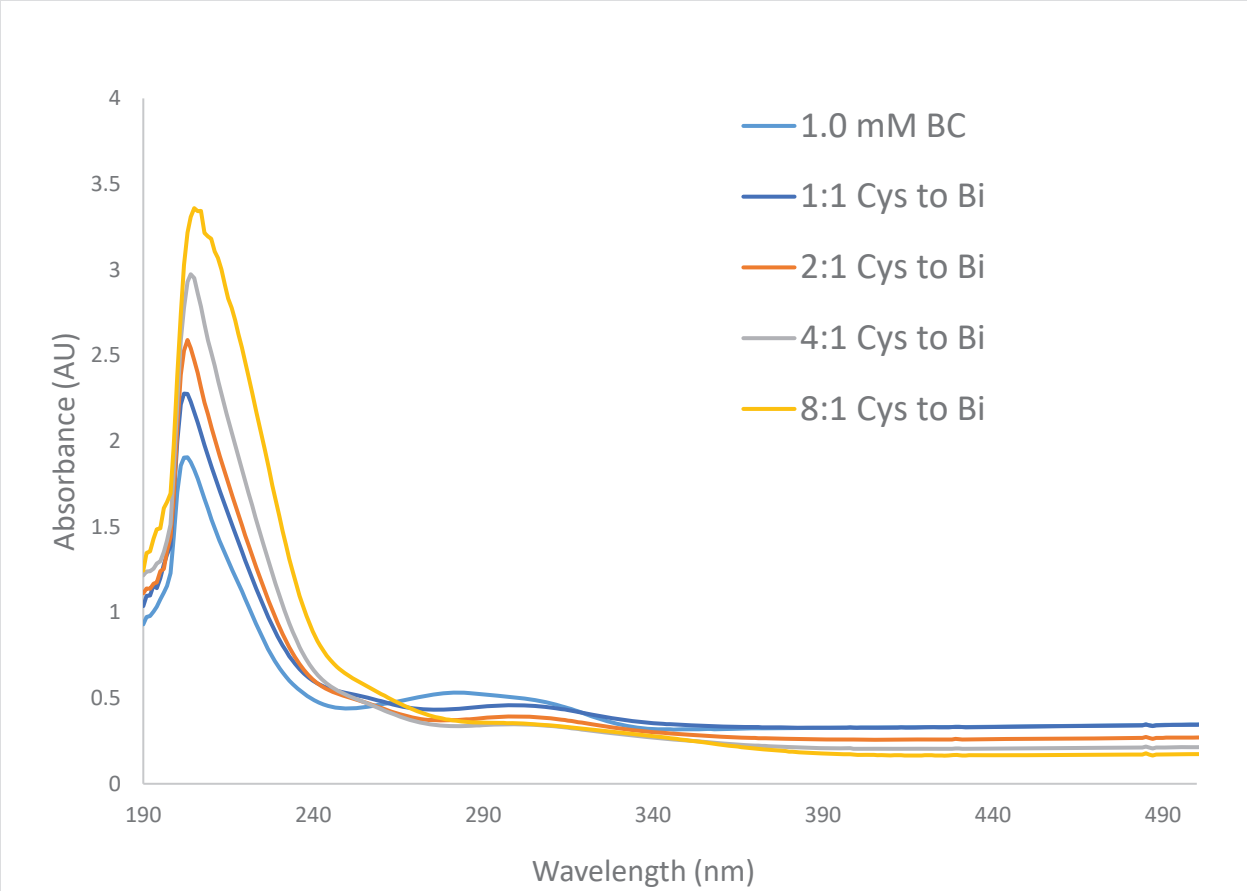

Figure 34. UV-Vis spectra of 1.0 mM BC in 0.10 M HCl, with incremental additions of L-cysteine. The path length was 1.00 cm.

Bismuth(III) citrate (BC) in pH 1.0 HNO_3, with L-cysteine additions

At the same pH value of 1.0 but without the possibility of chloride complexation, 1.0 mM BC was also studied in pH 1.0 HNO_3. The cyclic voltammogram showed that successive of L-cysteine additions caused increases in the reduction peak current, indicating that more bismuth has gone into solution (Figure 35). However, due to the lack of bismuth reduction peak potential shifts upon additions of L-cysteine, it is apparent that cysteine does not undergo strong interactions with BC. The UV-Vis spectrum in Figure 36 shows mostly an intact bismuth citrate band at 263 nm as L-cysteine was added, with an accompanying weak response at 350 nm due to interaction between bismuth and L-cysteine. This indicates that L-cysteine does play a role in complexation in pH 1.0 HNO_3, but the low intensity of the band at 350 nm compared to that in previous work (21) suggests that that L-cysteine is not a strong ligand in this case. The tridentate citrate ligand is evidently strong enough in both pH 1.0 HCl and HNO_3 that it continues to remain complexed with bismuth

even as L-cysteine is added, although the extent of complexation is greater at 0.10 M HNO_3 than in 0.10 M HCl.

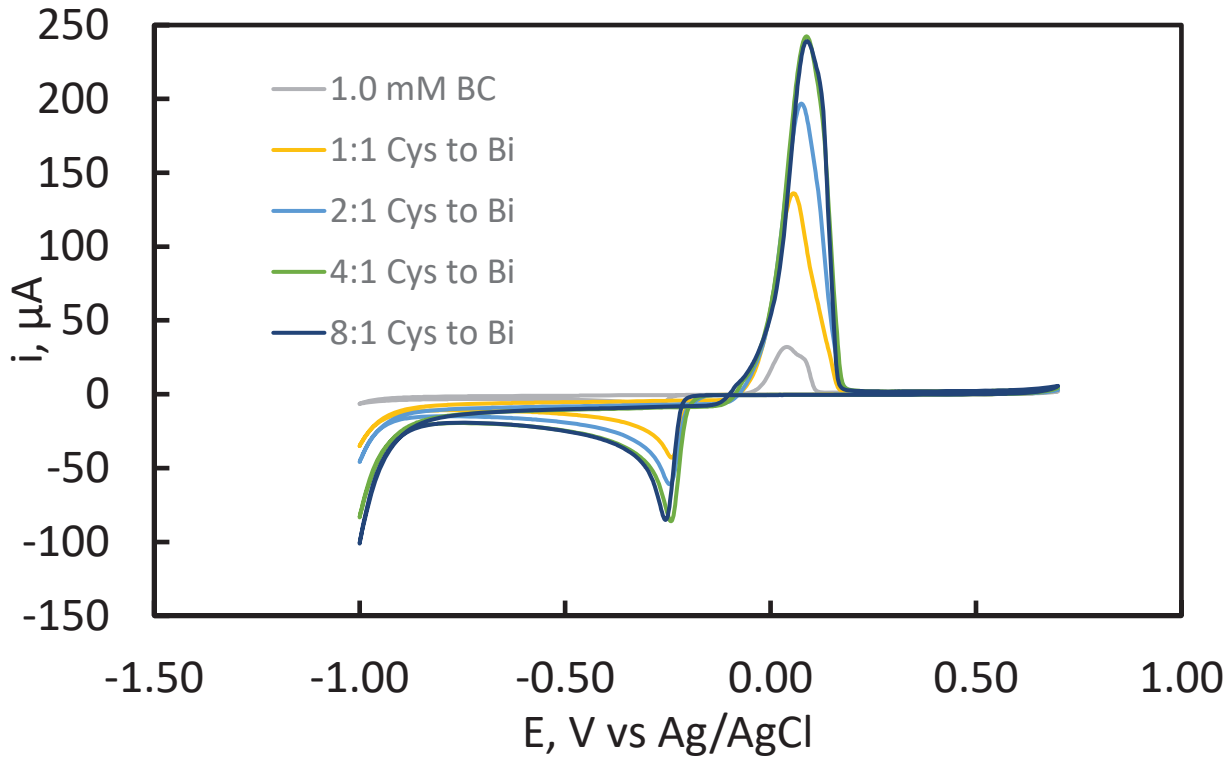

Figure 35. Cyclic voltammograms for 1.0 mM BC at glassy carbon in 0.10 M HNO_3, 100 mV/s, showing the effects of L-cysteine additions.

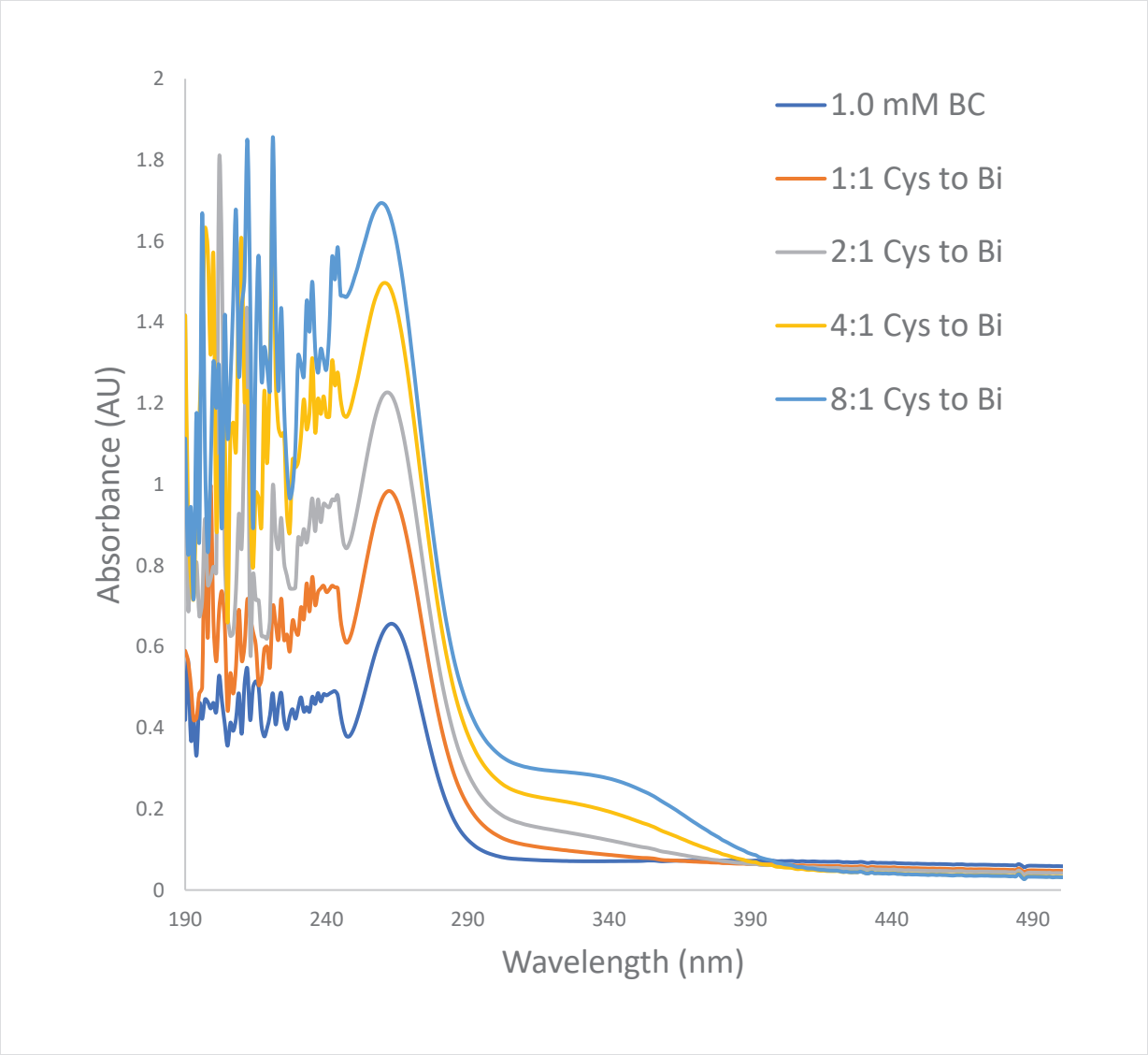

Figure 36. UV-Vis spectra of 1.0 mM BC in 0.10 M HNO_3, with incremental additions of L-cysteine. The path length was 1.00 cm.

Bismuth(III) citrate (BC) in pH 3.0 HCl, with L-cysteine additions

At more dilute levels in HCl, L-cysteine was able to interact more strongly than at pH 1.0 HCl. Initially, there is not much initial reduction current for the BC added to the pH 3.0 HCl solution. The much lower chloride content apparently does not allow the displacement of citrate from the BC complex. Subsequent additions of L-cysteine increased the current by bringing more of the bismuth into solution until it reaches a max current at 8:1 Cys to Bi (Figure 37). The peak currents generated from these conditions are greater than the peak currents generated from the sample in pH 1.0 HCl. While most ratios of Cys to Bi result in similar potential shifts, the 4:1 Cys

to Bi sample had a slightly more positive reduction potential. The cause of that is unknown. However, the UV-Vis spectra confirmed the complexation between L-cysteine and bismuth due to the formation of a 350 nm peak (Figure 38) having similar absorbance to that found in previous work (21). Overall, the results of 1.0 mM BC in pH 3.0 HCl with L-cysteine additions show that L-cysteine complexation is not as extensive as it is at pH 7.4, because it requires 8:1 Cys to Bi to form the complex versus the 2:1 Cys to Bi to form the complex in the pH 7.4 MOPS buffer (Figure 40). At pH 3.0, L-cysteine is more highly protonated than at pH 7.4, explaining the lowered effectiveness of L-cysteine as a ligand at pH 7.4.

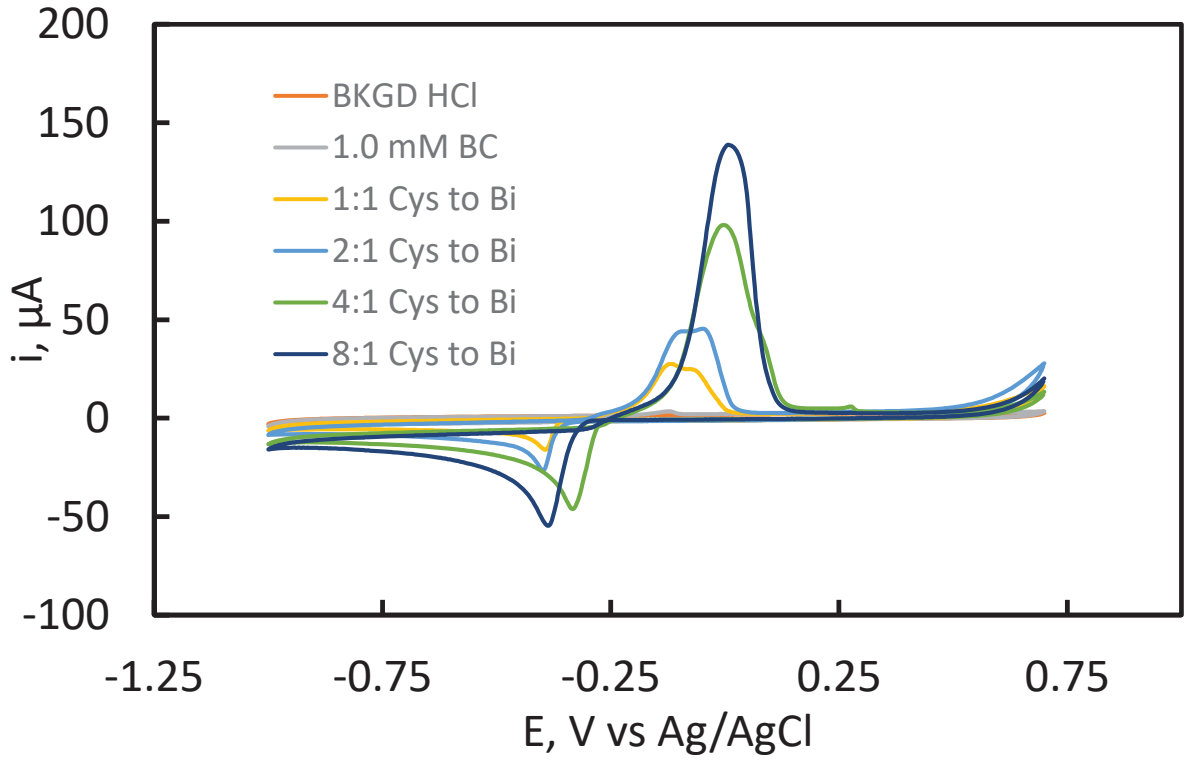

Figure 37. Cyclic voltammograms for 1.0 mM BC at glassy carbon in 1.0 x 10^{-3} M HCl (0.1 M ionic strength), 100 mV/s, showing the effects of L-cysteine additions.

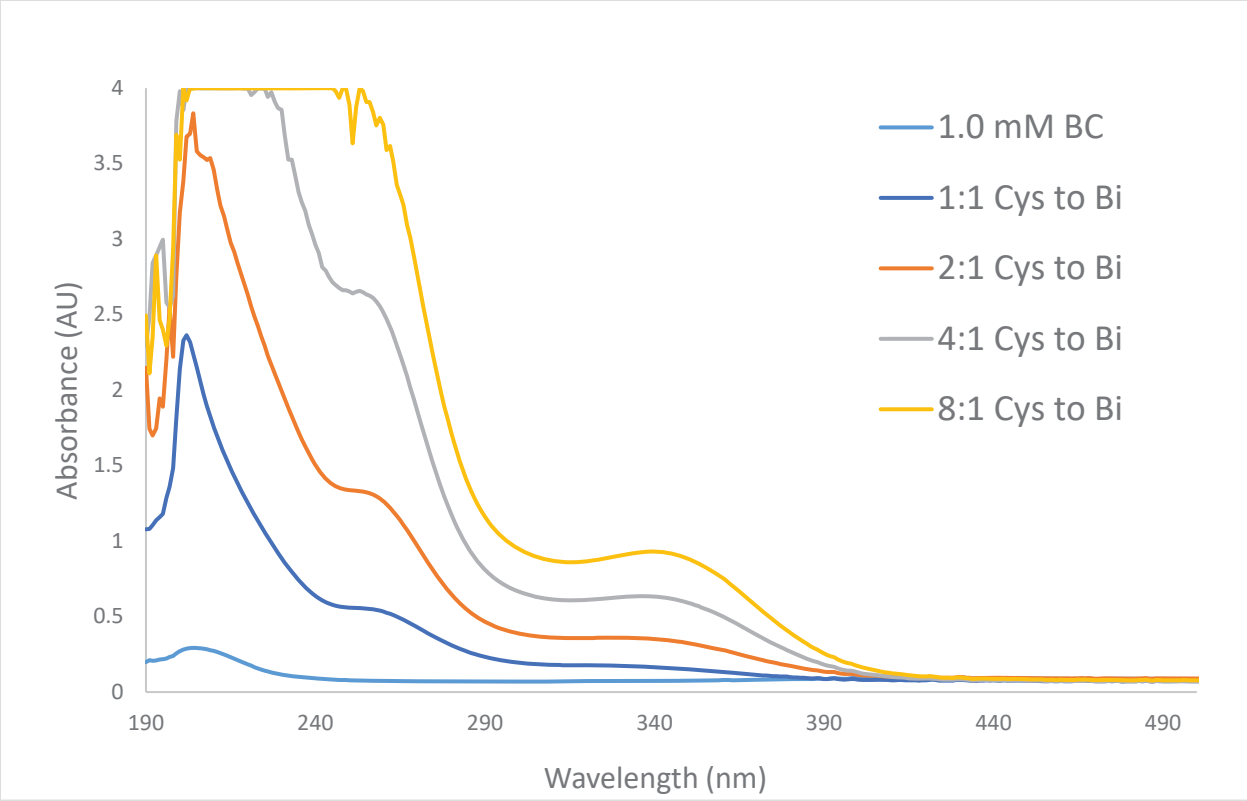

Figure 38. UV-Vis spectra of 1.0 mM BC in 1.0 x 10^{-3} M HCl (0.1 M ionic strength), with incremental additions of L-cysteine. The path length was 1.00 cm.

Bismuth(III) citrate (BC) in pH 7.40 MOPS buffer, with L-cysteine additions

The affinity of L-cysteine for bismuth at physiological conditions is shown by the various reduction peak potential shifts on the cyclic voltammograms (Figure 39). At 1:1 and 2:1 Cys to Bi, there is a reduction peak and a shoulder. Additionally, at 2:1 Cys to Bi the current reaches a maximum at around -100 μA, after which (4:1 and 8:1 Cys to Bi), the reduction potential and current become similar to each other. The presence of two reduction processes at the 1:1 and 2:1 points may be due to the presence of both citrate and L-cysteine as ligands around bismuth at this point in the addition sequence. Similarly, the UV-Vis spectra show that the complex is still forming at 1:1 and 2:1 with slight increases in absorbance at 320 nm (Figure 40). Going from 4:1 to 8:1, the absorbance signal does not change very much, indicating that the complex has fully formed at approximately the 2:1 point. However, the peaks at 320 nm vice the bismuth-cysteine complex peak at 340 suggests that there may still be a mixed complex, with citrate ligands still bonding some bismuth rather than cysteine being able to displace all of the ligands. Previous work did cite that cysteine is able to completely displace citrate in a 3:1 Cys to Bi ratio by X-ray diffraction and

UV-Vis spectroscopy (33). The bismuth stripping peak areas also support complexation at about the 2:1 Cys to Bi ratio, considering that the bismuth stripping peak areas are similar at the 2:1, 4:1, and the 8:1 Cys to Bi points. The larger reduction peak current for the 2:1 addition compared to those for the other additions is probably due to enhancement of this current by some surface interaction (adsorption) of the complex with the electrode. This explanation is supported by the similar stripping peak areas for curves beyond the 2:1 point. This behavior was also noted for BSS in pH 7.40 MOPS buffer (Figure 29). Finally, the changing profile of the stripping peaks is explained by the increasing concentration of excess L-cysteine in the solution, causing the stripping of bismuth to occur at less positive potentials as the L-cysteine concentration increases. Overall, the physiological condition allows for favorable interactions between BC and L-cysteine.

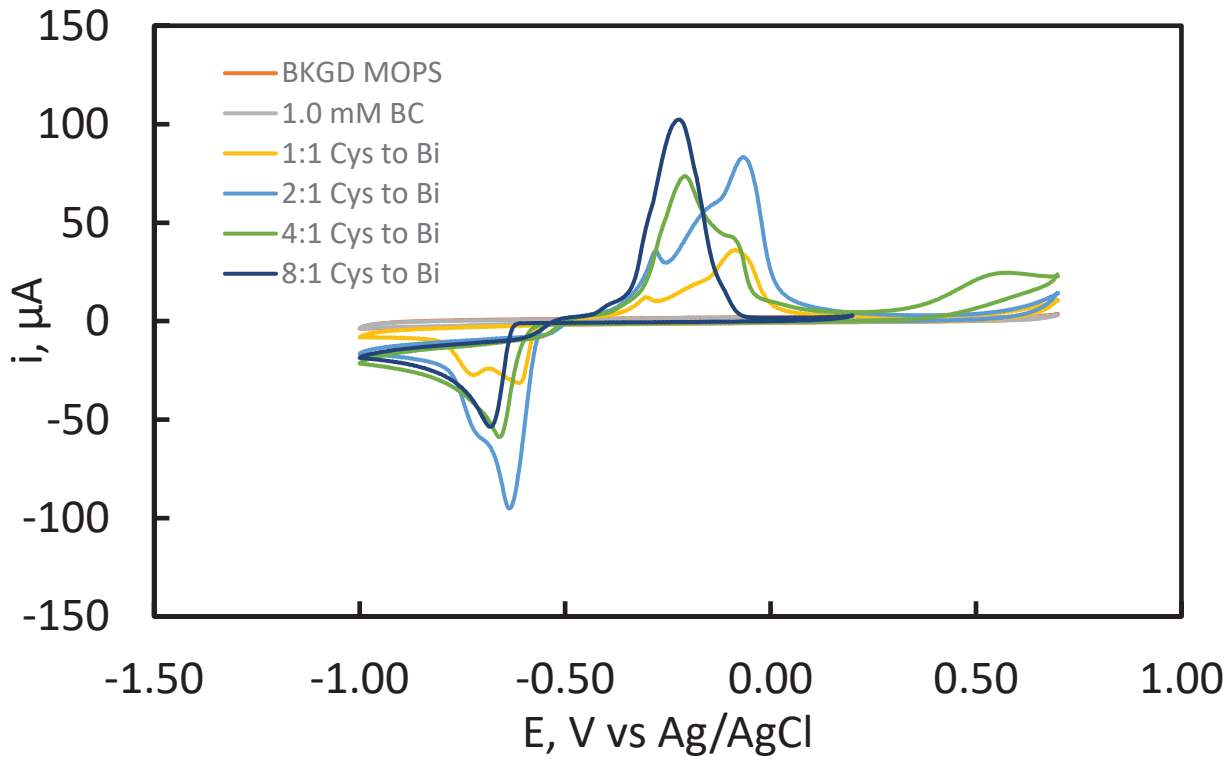

Figure 39. Cyclic voltammograms for 1.0 mM BC at glassy carbon in pH 7.40 MOPS buffer, 100 mV/s, showing the effects of L-cysteine additions.

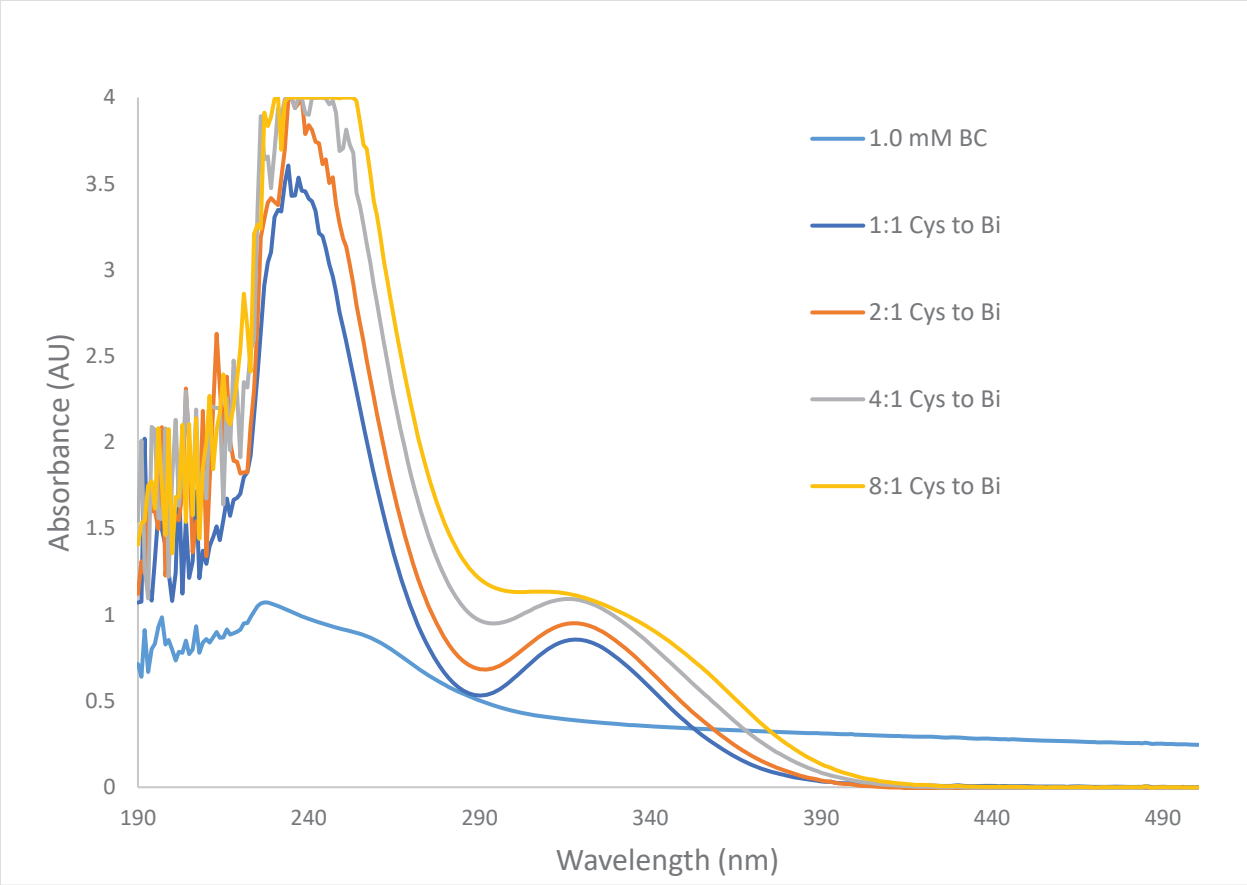

Figure 40. UV-Vis spectra of 1.0 mM BC in pH 7.40 MOPS buffer, with incremental additions of L-cysteine. The path length was 1.00 cm.

Conclusions

Bismuth compounds (bismuth(III) nitrate BN, bismuth(III) salicylate BSS, bismuth(III) citrate BC) were able to form soluble complexes with L-cysteine and L-glutathione under various conditions. However, it should be noted that for low pH environments (pH 1.00) with high proton or high chloride ion concentrations, the ability for bismuth-cysteine complexes to form is greatly hindered due to the fully protonated L-cysteine's lowered affinity for Bi(III). Diluted acid conditions (pH 3.00) did greatly improve L-cysteine's affinity for Bi(III), reaffirming the relationship between the different protonation states of this amino acid and its ability to form complexes with Bi(III). For instance, 1.0 mM BN in pH 1.0 HCl was unable to completely form a bismuth-cysteine complex due to the high proton and chloride levels. However, 1.0 mM BN in pH 3.0 HNO_3 and pH 3.0 HCl all showed evidence of complexation. 1.0 mM BSS had a much more difficult time complexing with L-cysteine in pH 1.0 and pH 3.0 HCl. The results of this show that the salicylate ligand has a greater affinity for Bi(III) in low pH than does L-cysteine. Conversely, at pH 7.40, L-cysteine was observed to interact with BSS, forming a soluble complex. Bismuth citrate seemed to have experienced the same result as BSS in low pH values. Due to high proton and chloride contents, the complete bismuth-cysteine complex was unable to form. Instead, at low pH values, a mixed complex with chloride ions may be present. Like BSS, BC is able to complex with L-cysteine at pH 7.40. This shows that L-cysteine has greater affinity for Bi(III) due to its lower state of protonation at higher pH values. The experiments are summarized by the table below:

Table 1. Summary of Experiments

Bismuth Species	Acidity	Added Ligand	Figures	Main Results
1.0 mM BN	pH 1.0 HCl	L-Cys	4, 5	mixed complex with chloride ions
	pH 1.0 HNO_3	L-Cys	6, 7	evidence of complexation
	pH 3.0 HNO_3	L-Cys	12, 13	evidence of complexation
	pH 3.0 HCl	L-Cys	14	evidence of complexation
	pH 7.4 MOPS	L-Cys	15	evidence of complexation
	pH 1.0 HCl	GSH	8, 9	mixed complex with chloride ions
	pH 1.0 HNO_3	GSH	10, 11	evidence of complexation
	pH 7.4 MOPS	GSH	16, 17, 18	evidence of complexation
1.0 mM BSS	pH 1.0 HNO_3	L-Cys	19, 20	difficulty in complexation
	pH 1.0 HCl	L-Cys	23, 24	difficulty in complexation
	pH 3.0 HCl	L-Cys	27, 28	evidence of complexation
	pH 7.4 MOPS	L-Cys	29, 30	evidence of complexation
	pH 1.0 HNO_3	GSH	21, 22	difficulty in complexation
	pH 1.0 HCl	GSH	25, 26	difficulty in complexation
	pH 7.4 MOPS	GSH	31, 32	evidence of complexation
1.0 mM BC	pH 1.0 HCl	L-Cys	33, 34	mixed complex with chloride ions
	pH 1.0 HNO_3	L-Cys	35, 36	difficulty in complexation
	pH 3.0 HCl	L-Cys	37, 38	evidence of complexation
	pH 7.4 MOPS	L-Cys	39, 40	evidence of complexation

Thus, bismuth-based drugs could potentially be designed to target areas of the body in physiological conditions to improve efficacy. In comparing the different sulfur-containing biomolecules, both L-cysteine and L-glutathione were able to form soluble complexes with the bismuth compounds mentioned above. The rate of the interactions between L-cysteine and L-glutathione, however, differed greatly. L-cysteine had a much faster reaction rate than L-glutathione, largely due to the differences in their respective molecular sizes. Nevertheless, the interactions between the sulfur-containing biomolecules and bismuth compounds that create soluble complexes lay an important framework for future bismuth metallodrug design. The challenges that need to be navigated in creating such drugs include increasing the solubility of compounds at low pH values and ensuring ligand size and interactions in the bismuth compounds are readily displaced by the sulfur-containing biomolecules in the body.

Future Work

For future work, more investigations will be done in a more dilute acidic environment (i.e. pH 3.0) to gain a larger scale at which these sulfur-containing biomolecules can operate. Additionally, investigations pertaining to the rates of reactions (i.e. kinetics) will be conducted to gain a sense of the magnitude of the time scale at which these complexes form, especially comparing the kinetics of L-cysteine versus L-glutathione. Finally, structures of these complexes will be determined in order to verify the stoichiometric ratio of ligands to bismuth ion in a fully formed complex. Methods for these processes include X-ray crystallography and NMR (nuclear magnetic resonance). Typically, for X-ray crystallography, a highly-ordered three-dimensional crystal of the bismuth-cysteine or bismuth-GSH complex is obtained and by directing a collimated X-ray beam through the sample, a structure can be determined by measuring the positions and amplitudes of X-rays diffracted from the sample, followed by computational refinement of a corresponding molecular model against the data. In contrast, NMR spectroscopy provides an atomic structure of the molecule in solution, based on distance couplings between adjacent chemical moieties deduced using radio region electromagnetic radiation.

References

1. Koegan, D.; Griffith, D. Current and potential applications of bismuth-based drugs. *Molecules* **2014,** *19* (9), 15258-15297.
2. Gaynor, D.; Griffith, D. The prevalence of metal-based drugs as therapeutic or diagnostic agents: Beyond platinum. *Dalton Transactions* **2012,** *41* (43), 13239-13257.
3. Salvador, J.; Figueiredo, S.; Pinto, R.; et al. Bismuth compounds in medicinal chemistry. *Future Med. Chem.* **2012,** *4* (11), 1495-1523.
4. DuPont, H. Bismuth subsalicylate in the treatment and prevention of diarrheal disease. *Drug Intel. Clin. Phar.* **1987,** *21* (9), 687-693.
5. Graham, D.; Lee, S. How to Effectively Use Bismuth Quadruple Therapy: The Good, the Bad, and the Ugly. *Gastroenterol. Clin. N.* **2015,** *44* (3), 537-563.
6. Rowinska-Zyrek M.; Witkowska, D.; Valensin, D.; et al. The C terminus of HspA— a potential target for native Ni(II) and Bi(III) anti-ulcer drugs. *Dalton Transactions* **2010,** *39* (25), 5814-5826.
7. Yang, N.; Tanner, J.; Zheng, B.; et al. Bismuth complexes inhibit the SARS coronavirus. *Angew Chem. Int. Ed. Engl.* **2007,** *46* (34), 6464-6468.
8. Wolf, D.; Wolf, C.; Rubin, D. Temporal Improvement of a COVID-19-Positive Crohn's Disease Patient Treated With Bismuth Subsalicylate. *Am. J. Gastroenterol.* **2020,** *115* (8), 1298.
9. Yuan, S.; Wang, R,; Chan, J.; et al. Metallodrug ranitidine bismuth citrate suppresses SARS-CoV-2 replication and relieves virus-associated pneumonia in Syrian hamsters. *Nat. Microbiol.* **2020,** *5* (11), 1439-1448.
10. Jin, L.; Szeto, K.; Zhang, L.; et al. Inhibition of alcohol dehydrogenase by bismuth. *J. Inorg. Biochem.* **2004,** *98* (8), 1331-1337.
11. Alkim et al. Role of Bismuth in the Eradication of *Helicobacter pylori*. *Am. J. Therapeutics* **2017,** *24* (6), 751-757.
12. Bland, M.; Ismail, S.; Heinemann, J.; et al. The action of bismuth against *Helicobacter pylori* mimics but is not caused by intracellular iron deprivation. *Antimicrob. Agents Ch.* **2004,** *48* (6), 1983-1988.
13. Busse, M.; Border, E.; Junk, P.; et al. Bismuth(III) complexes derived from α-amino acids: the impact of hydrolysis and oxido-cluster formation on their activity against Helicobacter pylori. *Dalton Transactions* **2014,** *43,* 17980.
14. Li, H.; Wang, R.; Sun, H. Systems Approaches for Unveiling the Mechanism of Action of Bismuth Drugs: New Medicinal Applications beyond *Helicobacter pylori* Infection. *Accounts, Chem. Res.* **2019,** *52* (1), 216-227.
15. Lambert, J.; Midolo, P. The actions of bismuth in the treatment of *Helicobacter pylori* infection. *Aliment Pharm. Therap.* **1997,** *11* (1), 27-33.
16. Rowinska-Zyrek M.; Witkowska, D.; Bielinska, S.; et al. The –Cys—Cys– motif in Helicobacter pylori's Hpn and HspA proteins is an essential anchoring site for metal ions. *Dalton Transactions* **2011,** *40*, 5604.

17. Hong, Y.; Lai, Y.; Chan, G.; et al. Glutathione and multidrug resistance protein transporter mediate a self-propelled disposal of bismuth in human cells. *P. Natl. Acad. Sci. USA.* **2015,** *112* (11), 3211-3216.
18. Cole, S.; Deeley, R. Transport of glutathione and glutathione conjugates by MRP1. *Trends Pharmacol. Sci.* **2006,** *27* (8), 438-446.
19. Leslie, E. Arsenic-glutathione conjugate transport by the human multidrug resistance proteins (MRPs/ABCCs). *J. Inorg. Biochem.* **2012,** 141-149.
20. Cheek, G,; Worosz, M.; Doan, M.; Clark, D. Electrochemical Studies of Zinc/L-Cysteine Interactions in Aqueous Buffers. *ECS Transactions* **2017,** *80,* 1159.
21. Cheek, G.; Pena, D. Electrochemical Investigations of L-Cysteine Interactions with Bismuth Ions. *J. Electrochem. Soc.* **2020,** *167* (15), 155522.
22. Sun, H.; Li, H.; Harvel, I.; et al. Interactions of bismuth complexes with metallothionein(II). *J. Bio. Chem.* **1999,** *274* (41), 29094-29101.
23. Adeyemi, J.; Onwudiwe, D. Chemistry of some biological potential of bismuth and antimony dithiocarbamate complexes. *Molecules* **2020,** *25* (2).
24. Briand, G.; Burford, N.; Eelman, M.; et al. Identification, isolation, and characterization of cysteinate and thioactate complexes of bismuth. *Inorg. Chem.* **2004,** *43* (20), 6495-6500.
25. Poole, L. The basics of thiols and cysteines in redox biology and chemistry. *Free Rad. Bio. and Med.* **2015,** *80*, 148-157.
26. Salder, P.; Sun, H.; Li, H. Bismuth(III) Complexes of the Tripeptide Glutathione (γ-L-Glu–L-Cys–Gly). *Chem. Eur. J.* **1996,** *2,* 701-708.
27. Harris, D.; Lucy, C. *Quantitative Chemical Analysis,* 9th ed.; W. H. Freeman and Company, 2016
28. Olmos, M. P.; Martinez, A. M.; Kazemi, R.; et al. Simultaneous Electrochemical Speciation of Oxidized and Reduced Glutathione. Redox Profiling of Oxidative Stress in Biological Fluids with a Modified Carbon Electrode. *Anal. Chem.* **2017,** *89* (20), 10726-10733.
29. Nelson, D.L., Cox, M.M., and Hoskins, A.A. *Lehninger Principles of Biochemistry,* 8th ed., Macmillan Learning, 2021; pp. 73.
30. M. Pourbaix. *Atlas of Electrochemical Equilibria in Aqueous Solutions*, p. 536, Pergamon Press, New York (1966).
31. Bard, A.J.; Faulkner, L.R. *Electrochemical Methods, Fundamentals and Applications*, 2nd ed.; John Wiley and Sons: New York, 2001.
32. Lazarini, F. Thermal dehydration of some basic bismuth nitrates. *Thermochimica Acta*. **1981,** *46* (1), 53-55.
33. Wang, Y.; Xu, L. pH-dependent displacement of [Bi(citrate)]- with cysteine: Synthesis, spectroscopic and X-ray crystallographic characterization of $Bi(cysteine)_3$. *J. Inorg. Biochem.* **2008,** *102* (4), 988-991.
34. C. M. H. Ferreira, I. S. S. Pinto, E. V. Soares, and H. M. V. M. Soares, *RSC Advances*, **5**(39), 30989 (2015).

Appendix (Nomenclature and Abbreviations)

Anti-leishmanial: The ability to treat the parasite that causes the disease Leishmaniasis

BC: Bismuth subcitrate, Bismuth(III) citrate

BN: Bismuth subnitrate, Bismuth(III) nitrate

BSS: Bismuth subsalicylate, Bismuth(III) salicylate

Complex: The close association of a metal ion with a ligand

Cys: L-cysteine

GSH: L-glutathione

Lewis Base: Molecules or ions that are able to donate their electron pairs to a Lewis Acid

Ligand: A molecule with the ability to act as a Lewis base

Oxidation: The loss of electrons in a species

pH: Short for potential of hydrogen. A measure of the concentration of hydrogen ions (protons) are in solution. A low pH indicates an acidic solution (high concentration of protons) and a high pH indicates a basic solution (low concentration of protons)

Reduction: The gain of electrons in a species

Redox Process: A collective term for an electrochemical process that involves reduction and oxidation

Thiol: Signifies a sulfur functional group (SH).